



Principal Investigator: Prof. Robert Pilawa-Podgurski

Bio: Robert Pilawa-Podgurski is currently an Associate Professor in the Electrical Engineering and Computer Sciences Department at the University of California, Berkeley. Previously, he was an Associate Professor in Electrical and Computer Engineering at the University of Illinois Urbana-Champaign. He received his BS, MEng, and PhD degrees from MIT. He performs research in the area of power electronics. His research interests include renewable energy applications, electric vehicles, energy harvesting, CMOS power management, high density and high efficiency power converters, and advanced control of power converters. Dr. Pilawa-Podgurski received the Chorafas Award for outstanding MIT EECS Master's thesis, the Google Faculty Research Award in 2013, and the 2014 Richard M. Bass Outstanding Young Power Electronics Engineer Award of the IEEE Power Electronics Society, given annually to one individual for outstanding contributions to the field of power electronics before the age of 35. In 2015, he received the Air Force Office of Scientific Research Young Investigator Award, the UIUC Dean's Award for Excellence in Research in 2016, the UIUC Campus Distinguished Promotion Award in 2017, and the UIUC ECE Ronald W. Pratt Faculty Outstanding Teaching Award in 2017. He was the 2018 recipient of the IEEE Education Society Mac E. Van Valkenburg Award given for outstanding contributions to teaching unusually early in ones career. In 2023, he received the UC Berkeley EECS Department Electrical Engineering Outstanding Teaching Award. He is co-author of fifteen IEEE prize papers.



Lab Members:



Dr. Nathan Ellis



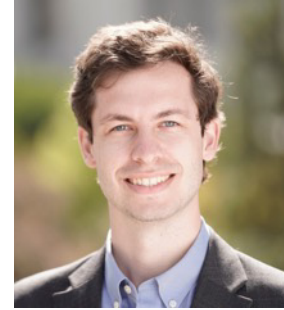
Dr. Samantha Coday



Margaret Blackwell



Rose Abramson



Nathan Brooks



Kelly Fernandez



Marrin Nerenberg



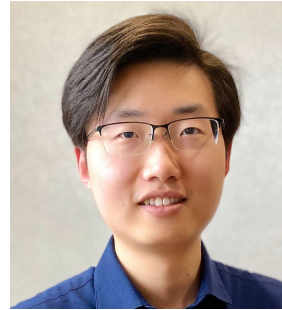
Logan Horowitz



Tahmid Mahbub



Rod Bayliss III



Yicheng Zhu



Rahul Iyer



Joseph Schaadt



Sahana Krishnan



Jiarui Zou



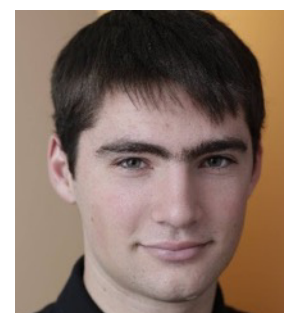
Haifah Sambo



Francesca Giardine



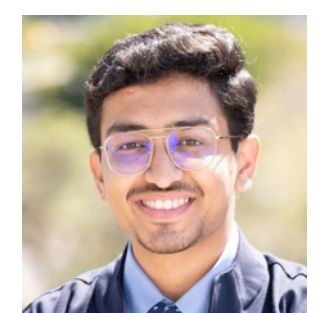
Ben Liao



Nathan Biesterfeld



Elisa Krause



Nagesh Patle

Ongoing Research Projects



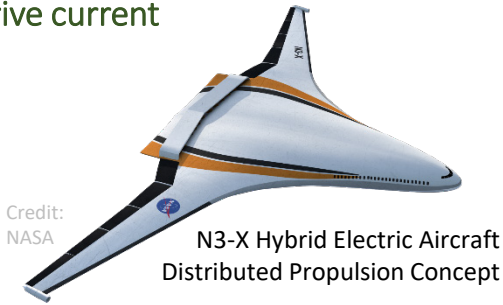
Extreme Performance Scalable Inverter Architecture for More Electric Aircraft (MEA) Propulsion



Berkeley Power and Energy Center

Motivation and Application

- Commercial aviation benefits from electric & hybrid vehicles
- Electric engines can be quieter and cleaner than jet engines
- Electric drive system must be **power-dense** and **efficient**
- Advanced power dense motors² need **low THD**, **high frequency** drive current



University of Illinois
1 MW Motor Concept²

NASA MEA Roadmap¹

NOx emissions

80%

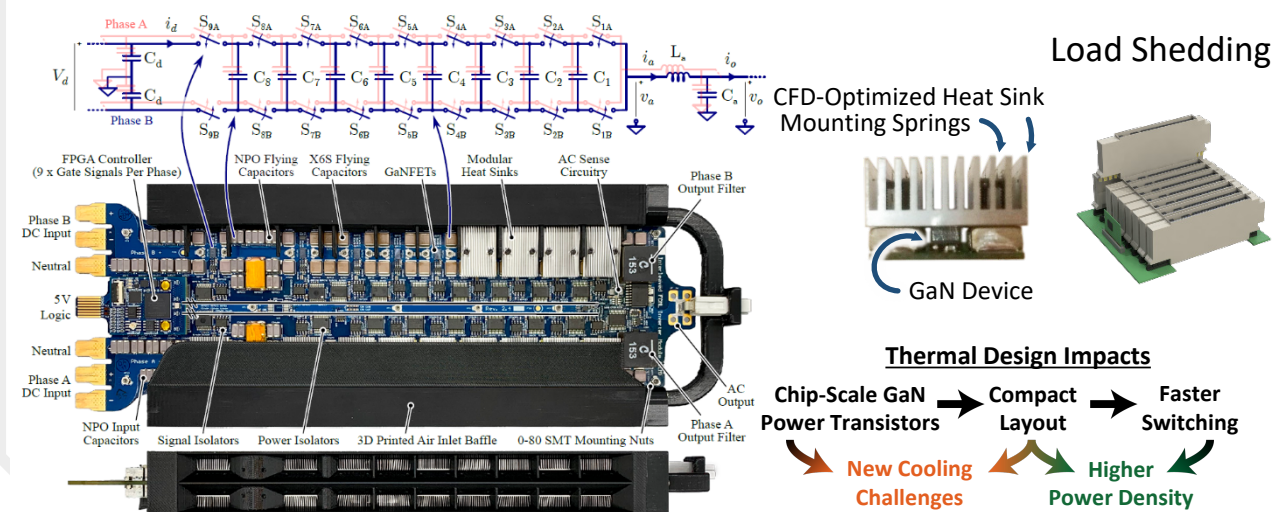
fuel consumption

60%

acoustic noise

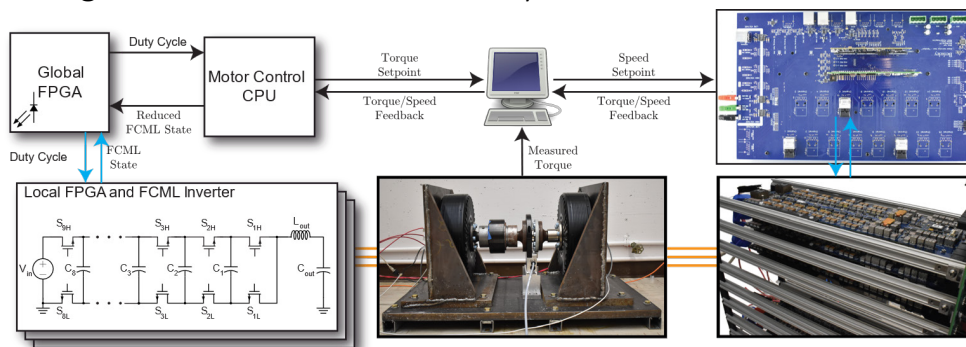
71dB

Electrical, Mechanical and Thermal Management Hardware



High Power Dynamometer

- Dyno incorporates two low-inductance Emrax 348 machines (peak power: 260 kW)
- Testing validated the Flying Capacitor Multilevel Converter's (FCML) strength in a realistic motor drive system



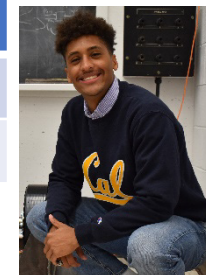
Experimental Verification or Other

- Prototype meets NASA performance metrics for turbo-electric aircraft⁴
- Integration of advanced thermal management will boost maximum output power and efficiency
- Modular design provides for power scalability and fault resiliency
- Next steps: verification of floating-point motor control algorithm and high-power dyno and next generation inverter hardware development

	NASA Target	This Work
Peak Efficiency	99%	98.95%
Power Density	19 kW/kg	38.4 kW/kg

References:

- N. Pallo, R. S. Bayliss and R. C. N. Pilawa-Podgurski, "A Multi-Phase Segmented Drive Comprising Arrayed Flying Capacitor Multi-Level Modules," IEEE APEC 2021
- N. Madavan, et al., "A NASA Perspective on Electric Propulsion Technologies for Commercial Aviation," 2016.
- X. Zhang and K. Haran, "High-Specific-Power Electric Machines for Electrified Transportation Applications Technology Options," IEEE ECCE 2016.
- N. Pallo, et al., "Power-Dense Multilevel Inverter Module using Interleaved GaN-Based Phases for Electric Aircraft Propulsion," IEEE APEC 2018.
- N. Pallo, C. Kharangate, et al., "Modular Heat Sink for Chip-Scale GaN Transistors in Multilevel Converters," IEEE APEC 2018.



Design of an Efficient, Lightweight Flying Capacitor Multilevel Converter for Electrified Flight

Motivation and Application

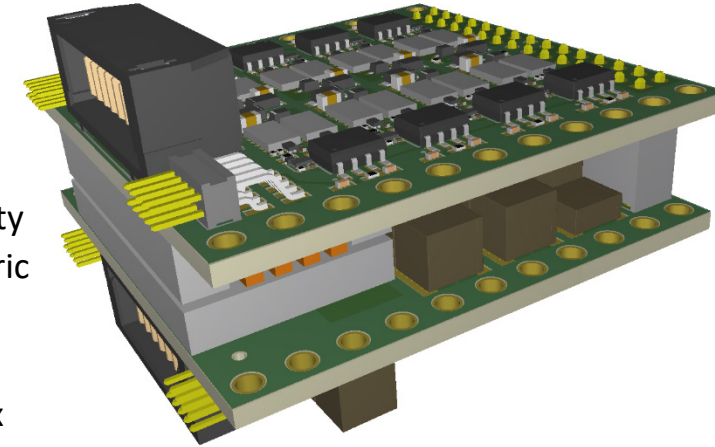


- Air travel accounts for ~200 million tons of CO₂ emissions annually (3% of US greenhouse gas emissions)^[1]
- Air travel demand is expected to double every fifteen years
- Electrification of flight requires efficient, lightweight, and reliable power conversion
- Hardware must be flight qualified

Pictured: Ampaire Electric EEL flight

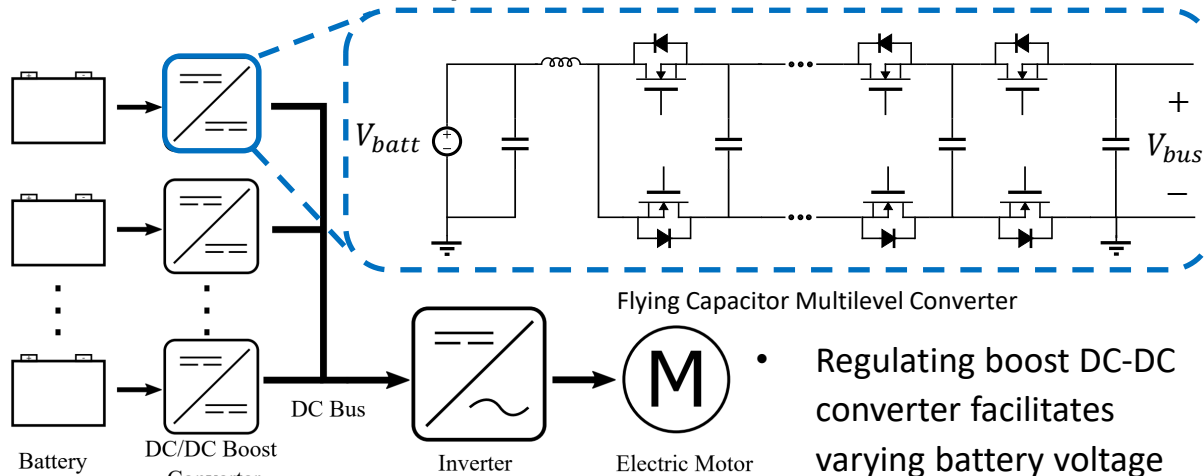
Hardware Prototype

- Snubbers enable decreased overlap loss without sacrificing conduction path
- Paralleled switches enable increased areal power density
- Derated energy density metric used to optimize flying capacitor part/count
- Custom inductor achieves 3x mass reduction



3D rendering of 8-level boost FCML prototype

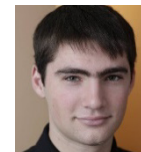
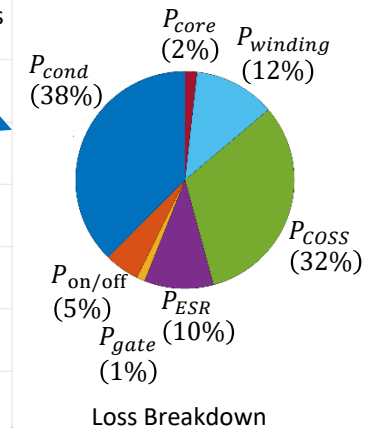
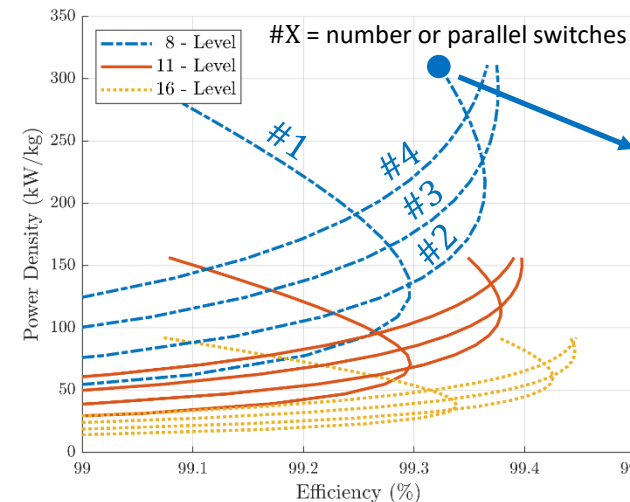
Proposed Solution



Electric Aircraft Drivetrain Architecture

Regulating boost DC-DC converter facilitates varying battery voltage and inverter load demand

Modeled Performance



Nathan Biesterfeld Email: biesterfeld@berkeley.edu
 Nathan Miles Ellis Email: nathanmilesellis@berkeley.edu
 Rahul Iyer Email: rkiyer@berkeley.edu

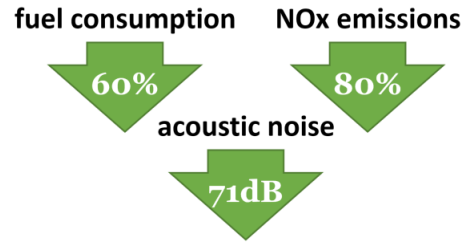
[1] <https://www.epa.gov/greenvehicles/fast-facts-transportation-greenhouse-gas-emissions>

Empowering Future Electric Aircraft with a Flying Capacitor Multilevel Inverter Utilizing Optimal Passive Components

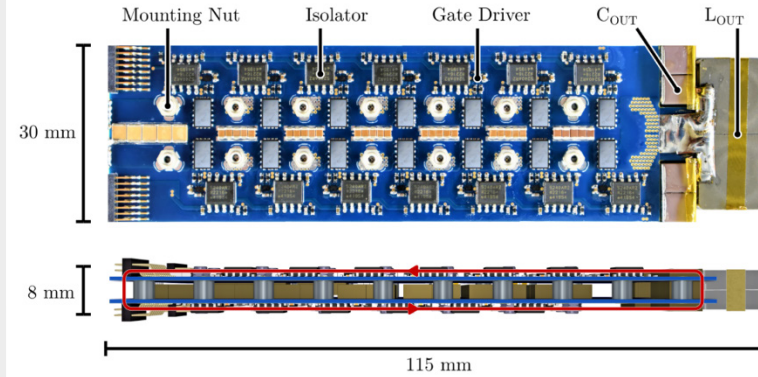


Motivation and Application

- Air travel accounts for ~200 million tons of CO₂ emissions annually (3% of US greenhouse gas emissions)^[1]
- Air travel demand doubles every fifteen years
- Electrification of flight requires efficient, lightweight, and reliable power conversion



Hardware Prototype

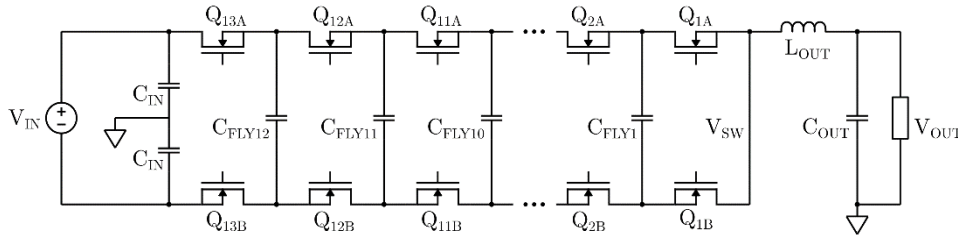


- 10 kW, 800 V, 14-level FCML
- Sandwich-style layout with two printed circuit boards
- Ultra-thin design, only 8 mm thick!

Key Converter Parameters	
Input Voltage	800 V _{DC}
Output Voltage	270 V _{RMS}
Effective Switching Frequency	1.95 MHz
Peak Output Power	10.3 kW
Peak Overall Efficiency	98.2 %
Gravimetric Density	170 kW/kg
Volumetric Density	370 kW/L

FCML with Optimal Passive Component Selection

Simplified 14-level FCML schematic



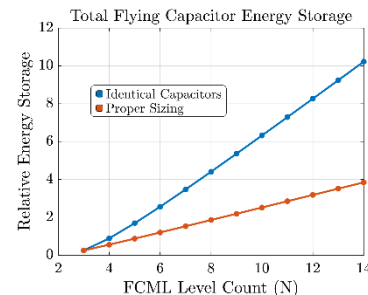
Capacitor Sizing

- Conventional approach utilizes large, identical capacitors
- Proposed approach optimally selects unique capacitors for each flying capacitance
- Enables > 50% reduction in size

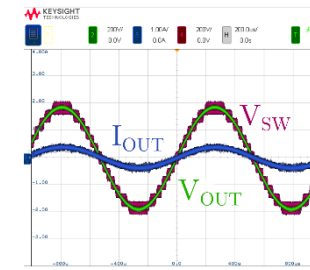
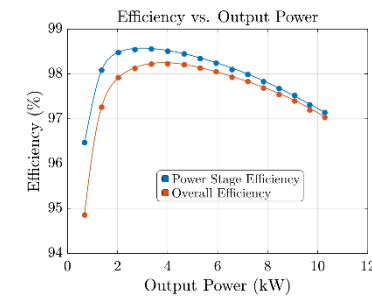
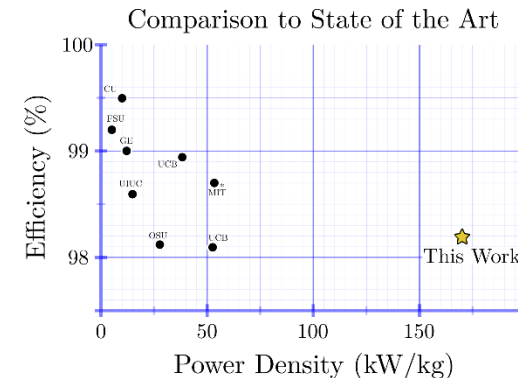


C₁₂
250 mJ

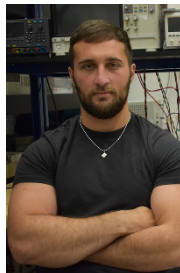
C₁
2 mJ



Experimental Verification



- Highest power density among state-of-the-art aircraft inverters
- Excellent capacitor balancing and low output distortion despite the small size of the converter



References:

[1] <https://www.epa.gov/greenvehicles/fast-facts-transportation-greenhouse-gas-emissions>

Tethered Power Systems for Lunar Mobility and Power Transmission (TYMPO)



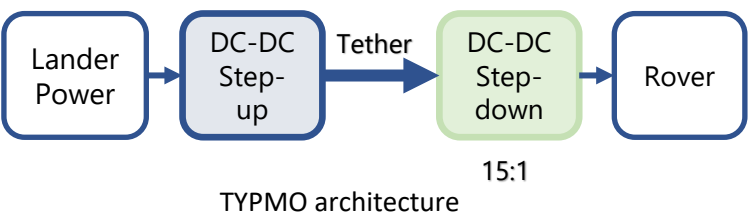
Berkeley Power and Energy Center

Motivation and Application

Extreme terrain capable robots will enable further exploration on sites such as pits on the moon and Martian landscape. Tethered power systems have been proposed to power these small rovers; however, they require high voltage DC power [1].

Challenges

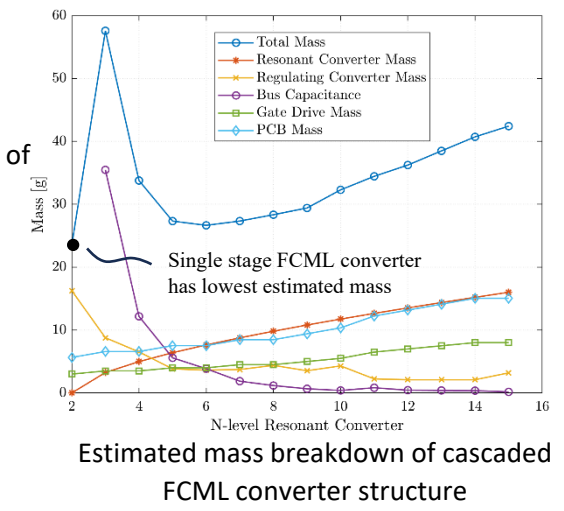
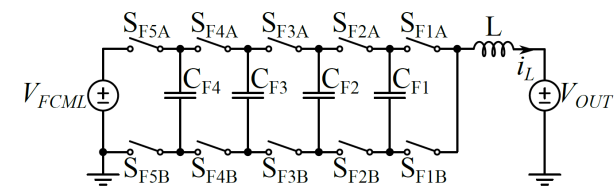
High voltage switches are difficult to use in space due to radiation effects. Additionally, the high voltage conversion ratio makes it difficult to design a compact and efficient power converter. Therefore, multilevel topologies offer promising solutions [2].



Tethered rover to explore lunar pits

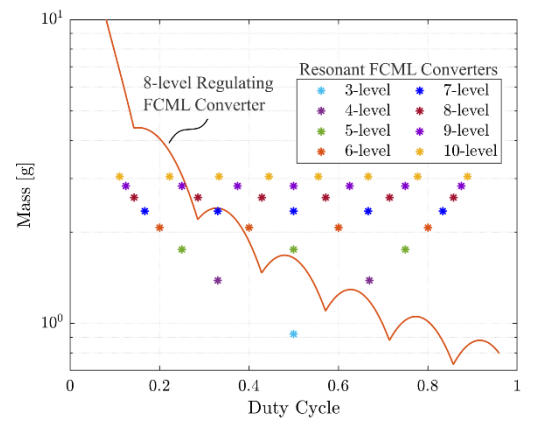
System Architecture (Flying Capacitor Multilevel Converter)

- Comparison of cascaded structure consisting of resonant flying capacitor multilevel converter (FCML) and regulating FCML (resonant FCML + regulating FCML) vs single-stage FCML converter
- Bus capacitance requirement diminishes benefits of cascaded structure



Passive Mass Minimization

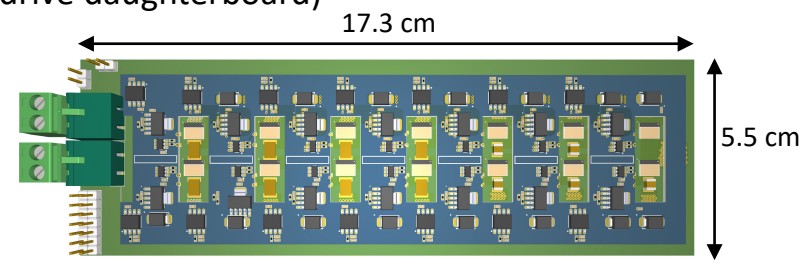
- Comparison of 8-level regulating mode FCML converter with a resonant mode FCML converter, demonstrating the advantages of a resonant converter in terms of passive component mass
- Each converter operating point is optimized for minimal mass based on the peak energy storage requirements of the passive components



Hardware Verification

840 V-to-120 V space-rated FCML converter to verify:

- PCB structure (Gate drive daughterboard)
- Part selection
- Thermal solutions
- Mass optimization



Student: Elisa Krause, Maggie Blackwell, Logan Horowitz
 Email: {elisa_krause, blackwell, logan_h_horowitz}@berkeley.edu

References:
 [1] P. McGarey, W. Reid and I. Nenas, "Towards Articulated Mobility and Efficient Docking for the DuAxel Tethered Robot System," 2019 IEEE Aerospace Conference, 2019, pp. 1-9.
 [2] P. McGarey, T. Nguyen, T. Pailevanian and I. Nenas, "Design and Test of an Electromechanical Rover Tether for the Exploration of Vertical Lunar Pits," 2020 IEEE Aerospace Conference, 2020, pp. 1-10.
 [3] S. Coday, A. Barchowsky and R. C. N. Pilawa-Podgurski, "A 10-level GaN-based Flying Capacitor Multilevel Boost Converter for Radiation-Hardened Operation in Space Applications," 2021 IEEE Applied Power Electronics Conference and Exposition (APEC), 2021, pp. 2798-2803.

On the Size and Weight of Passive Components: Scaling Trends for High-Density Power Converter Designs

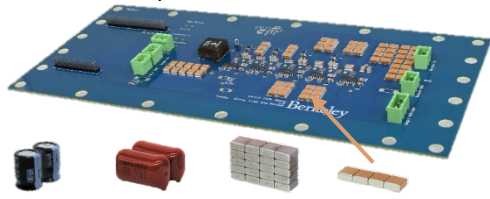


Berkeley Power and Energy Center

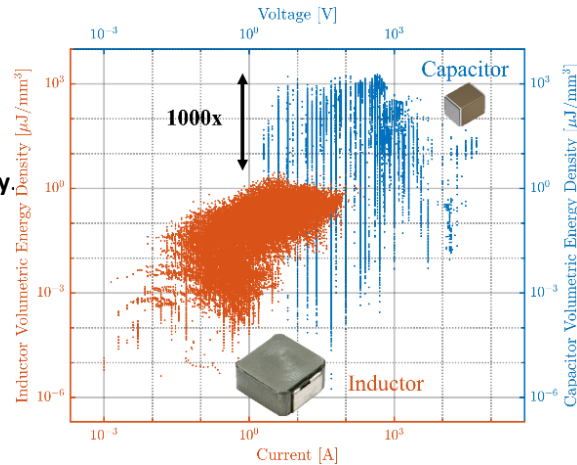
Motivation and Application

To build a high-density power converter, practicing engineers need to use passive components with the highest density.

- A component survey finds **Volumetric Energy Density**.
 - Visualized to assist component selection.
- But how to estimate **Gravimetric Energy Density**?
 - No component mass on most datasheet.

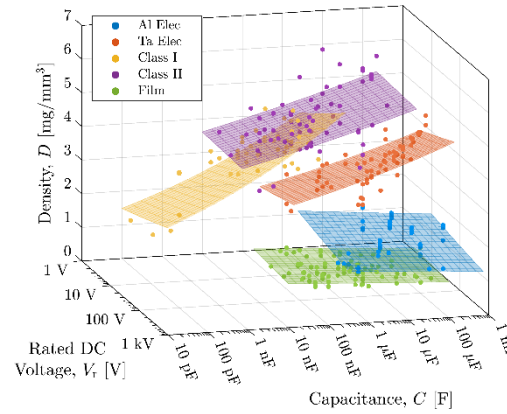


- | | | | |
|---|--|---|---|
| 2 μF @ 450 V
Aluminum
Electrolytic | 2 μF @ 450 V
Polypropylene
Metalized Film | 2 μF @ 450 V
Class 1
Ceramic | 2 μF @ 450 V
Class 2
Ceramic |
|---|--|---|---|



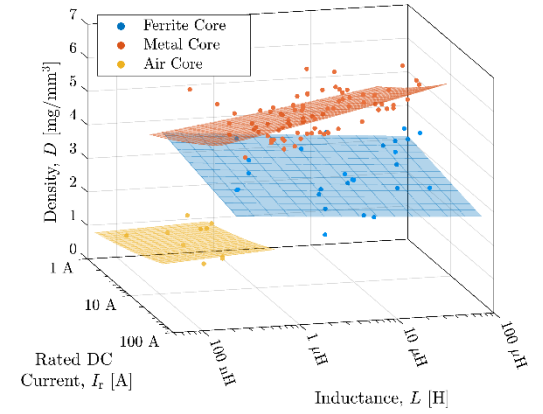
Volumetric Energy Density determined by a component survey encompassing over **606,000 capacitors** and **88,000 inductors**

Power Fit Estimation for Specific Density (D)



$$D = k \cdot V_r^\alpha \cdot C^\beta \left[\frac{\text{mg}}{\text{mm}^3} \right]$$

Mass data was obtained through manual measurements of over **6,000 components**



$$D = k \cdot I_r^\alpha \cdot L^\beta \left[\frac{\text{mg}}{\text{mm}^3} \right]$$

Capacitor Volumetric vs. Gravimetric Energy Density

$$\rho_v = \frac{1}{2} C V_r^2 = \left[\frac{\text{J}}{\text{mm}^3} \right]$$

Volumetric Energy Density

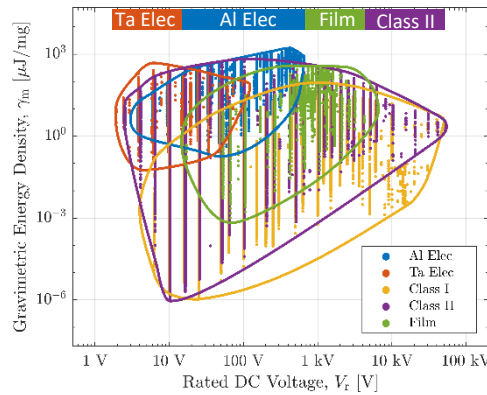
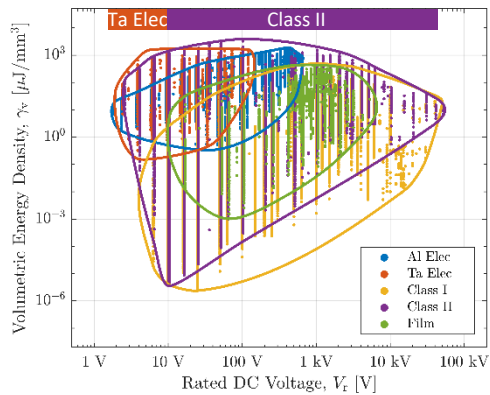
$$D(V_r, C) = \frac{\text{Mass}}{\text{Vol}}$$

$$\rho_m = \frac{1}{2} C V_r^2 = \left[\frac{\text{J}}{\text{mg}} \right]$$

Gravimetric Energy Density



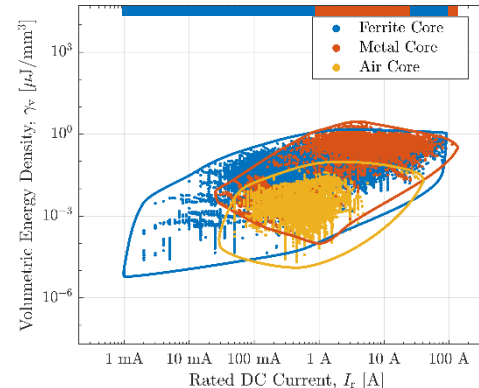
$$\frac{1}{D(V_r, C)}$$



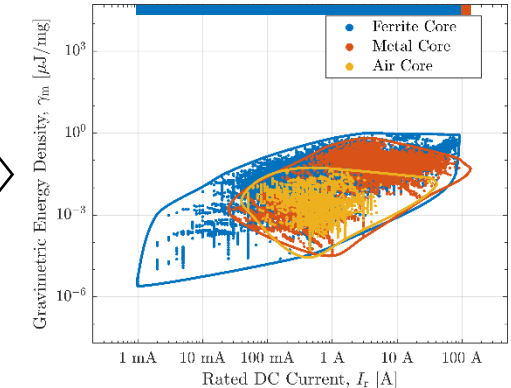
Use **Specific Density (D)** to Derive **Gravimetric Energy Density** from **Volumetric Energy Density**

Inductor Volumetric vs. Gravimetric Energy Density

Volumetric Energy Density

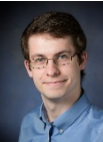


Gravimetric Energy Density



References: J. Zou, N. C. Brooks, S. Coday, N. M. Ellis and R. C. N. Pilawa-Podgurski, "On the Size and Weight of Passive Components: Scaling Trends for High-Density Power Converter Designs," 2022 IEEE 23rd Workshop on Control and Modeling for Power Electronics (COMPEL), Tel Aviv, Israel, 2022, pp. 1-7, doi: 10.1109/COMPEL53829.2022.9829957.

Jiarui Zou, jiarui.zou@berkeley.edu; Nathan Brooks, nathanbrooks@berkeley.edu; Samantha Coday, scoday@berkeley.edu; Nathan Ellis, Nathanmilesellis@berkeley.edu



Enabling Buck-Type AC/DC Grid-Tied Rectifiers Using Flying Capacitor Multi-Level Converters with Advanced Control



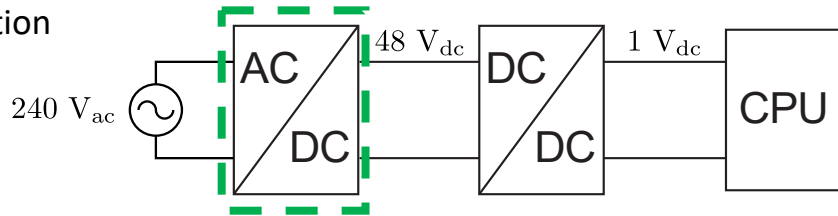
Motivation and Application

Data center power consumption
1%+ of global electricity demand
and growing [1]

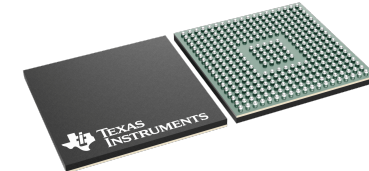
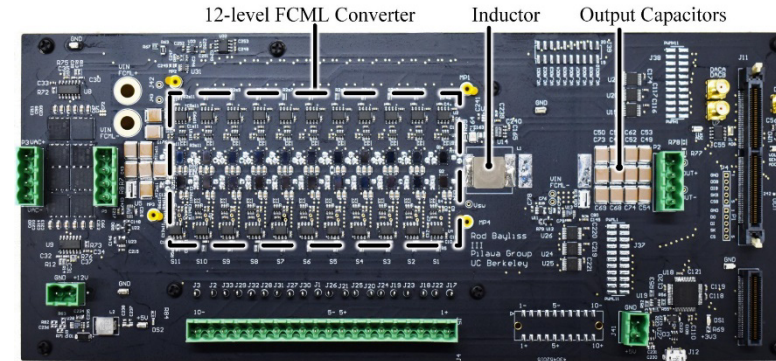


Single-stage rectification

- Increased efficiency
- Greater power density



Hardware



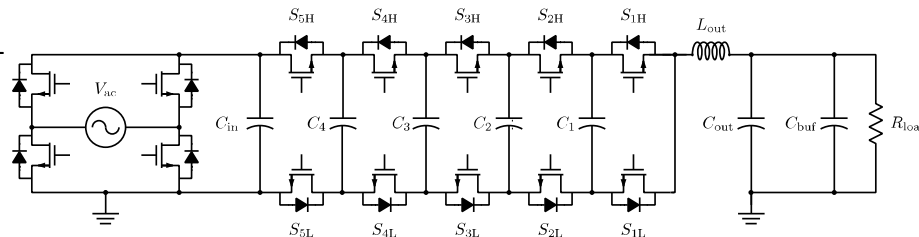
TI C2000 DSP (F28379D)

- 12-level prototype reconfigured as 5-level converter
- Flying capacitor voltages measured with non-isolated instrumentation amplifier

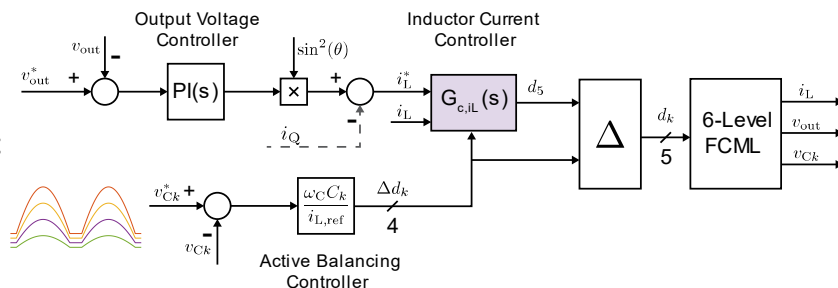
FCML and Active Flying Capacitor Voltage Balancing

6-Level Buck-Type FCML PFC Rectifier

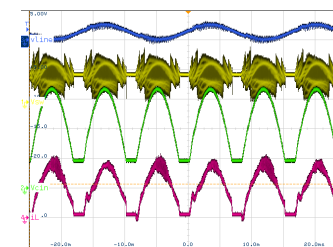
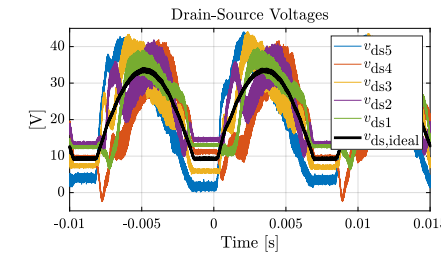
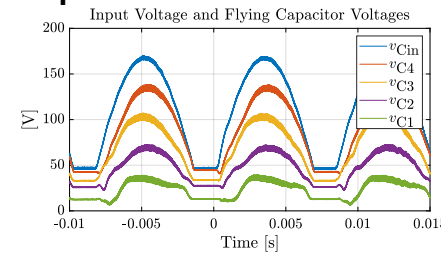
- Reduced magnetics volume
- High FOM switches



Control Schematic



Experimental Verification



Power Factor

Target	0.97
Passive Balancing	0.88
Active Balancing	0.97+

- Switch voltage stress limited → low voltage switches ✓
- High power factor input current achieved ✓

References:

[1] N. Jones, "The Information Factories," Nature 2018

Rod Bayliss III Email: rodbay@berkeley.edu



A 1200-A/48-V-to-1-V Switching Bus Converter: Toward Single-Stage Vertical Power Delivery for Next-Generation Ultra-High-Power Microprocessors

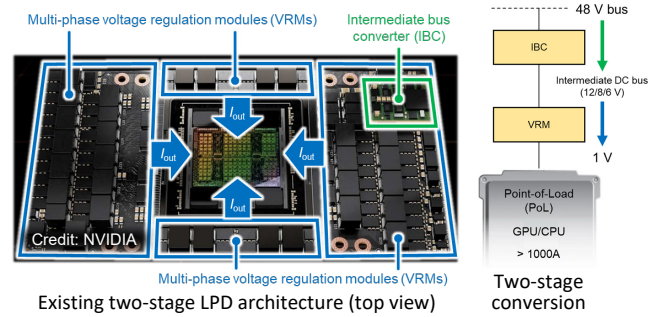


Berkeley Power and Energy Center

Background and Motivation

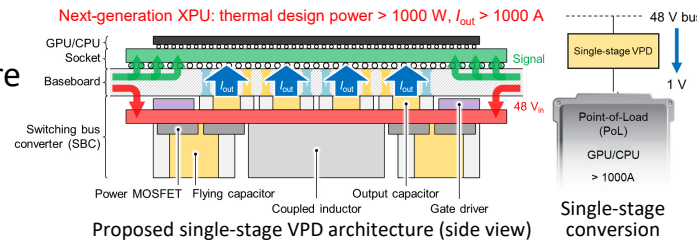
Existing two-stage lateral power delivery (LPD) architecture

- Large power distribution network (PDN) and high PDN losses
- Occupies a large area on the top side of the baseboard



Proposed single-stage vertical power delivery (VPD) architecture

- Much lower PDN losses
- Saves the topside area for high-speed communication and memories



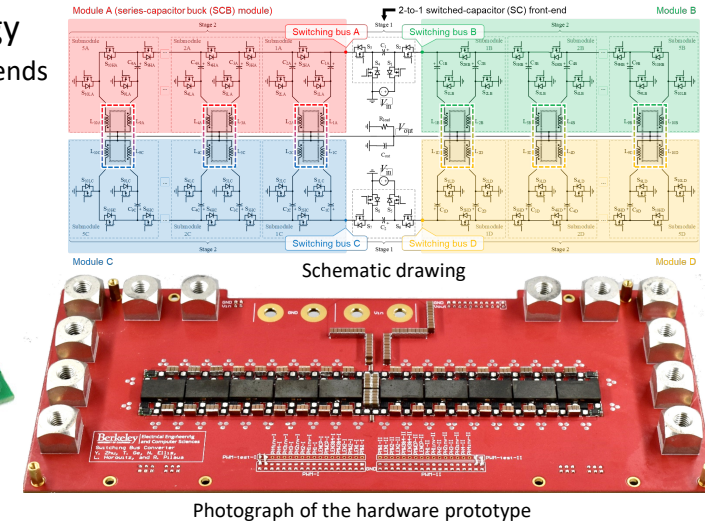
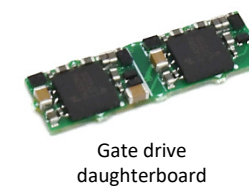
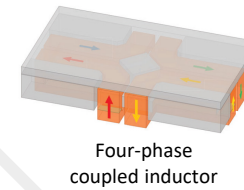
Proposed Switching Bus Converter (SBC)

Hybrid switched-capacitor topology

- Two 2-to-1 switched-capacitor (SC) front-ends
- Four series-capacitor buck (SCB) modules
- Two switching buses

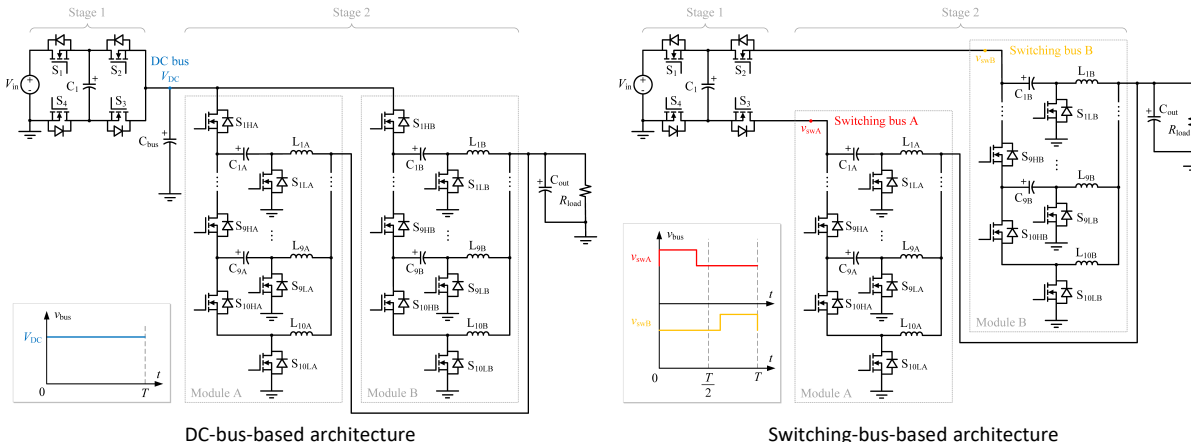
Hardware prototype

- Good modularity
- Custom four-phase coupled inductor
- Efficient and compact gate drive circuitry



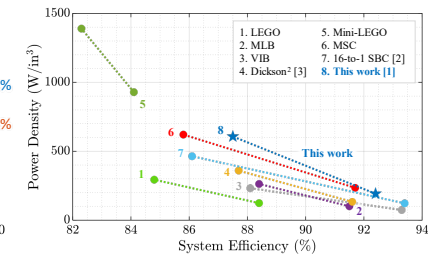
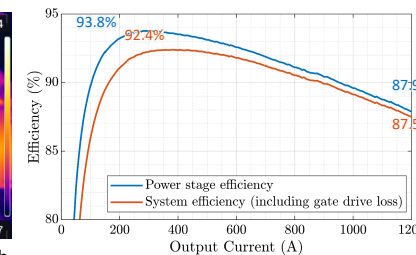
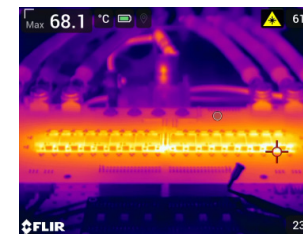
Advantages of Switching-Bus-Based Architecture

- Does not require a large decoupling capacitor to maintain a stiff DC bus voltage
- One redundant switch can be removed on each switching bus while two stages are merged
- Ensures complete soft-charging operation



Experimental Results and Performance Comparison

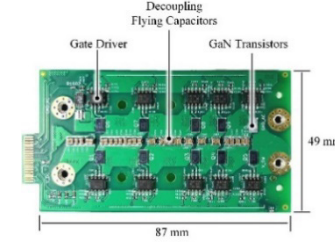
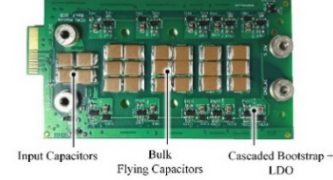
- 92.4% peak system efficiency and 607 W/in³ power density (including gate drive loss and volume)



References:

- [1] Y. Zhu, et al., "A 48-V-to-1-V Switching Bus Converter for Ultra-High-Current Applications," COMPEL 2023. **[Best Paper Award]**
- [2] Y. Zhu, et al., "A 500-A/48-to-1-V Switching Bus Converter: A Hybrid Switched-Capacitor Voltage Regulator with 94.7% Peak Efficiency and 464-W/in³ Power Density," APEC 2023.
- [3] Y. Zhu, et al., "A Dickson-Squared Hybrid Switched-Capacitor Converter for Direct 48 V to Point-of-Load Conversion," APEC 2022.

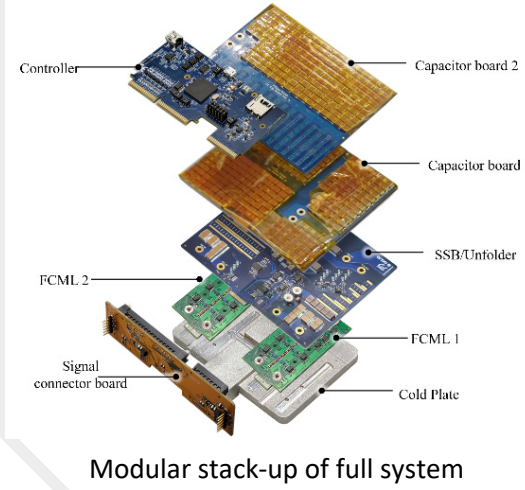




Flying capacitor multi-level (FCML) converter as the power factor correction stage

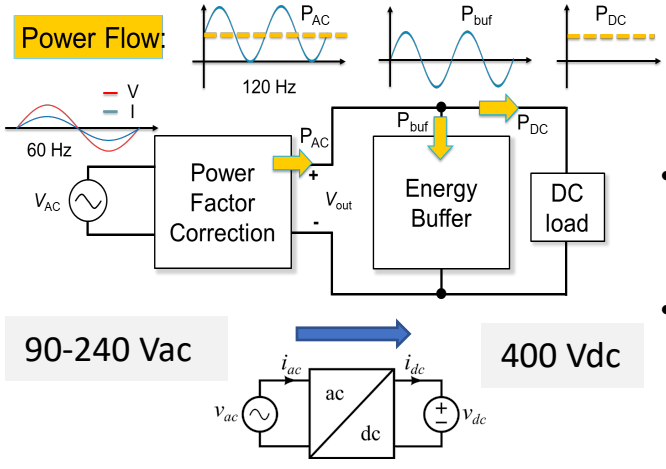
- Use of flying capacitors as energy storage greatly decreases volume of passive components and reduce filtering needs
- Series-stacked Buffer as energy buffer stage
- Use of active circuitry decreases capacitance requirement for twice-line frequency buffering and further promoted volume reduction

Hardware Implementation



Modular stack-up of full system

Motivation and Application

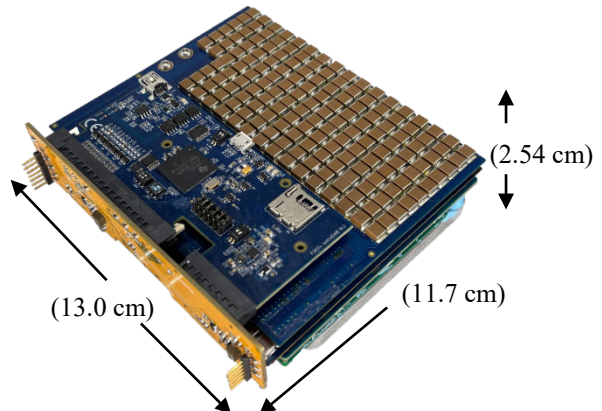


- 90-240 Vac to 400 Vdc is a critical conversion stage for applications such as data center power delivery, electric vehicle charging, etc.
- Ac-dc power factor correction
 - Reduce boost inductor size
- Twice-line frequency power ripple buffering
 - Reduce buffer capacitor size

Design Objectives

High Power Density

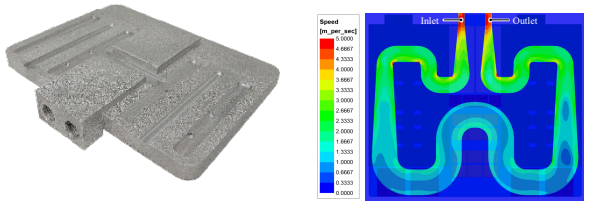
Reduce system volume via new circuit topologies and control



Reduced Weight

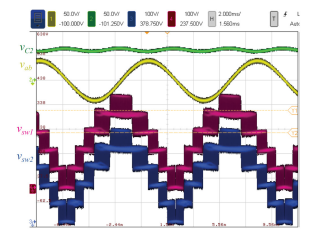
Custom 3D-printed cold-plate (collaboration with Miljkovic Group at UIUC)

3D printed cold-plate Printed Fluid Channels

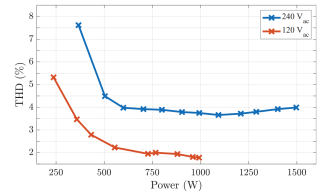


Experimental Verification

Parameter	Notes
Peak tested power	6.1 kW
Peak efficiency (1.1 kW)	99.1%
Efficiency @ 6.1 kW	97.8%
PFC up to 1.5 kW	> 99.6%
Box-volume power density with cold plate:	7.6 kW/L



400 V_{dc} to 240 V_{ac} system waveforms at 6.1 kW



THD up to 1.5 kW



Kelly Fernandez, Rahul Iyer, Jiarui Zou Email: kfernandez@berkeley.edu, rkiver@berkeley.edu, Jiarui.zou@berkeley.edu

References:

- [1] D. Chou et al., "An Interleaved 6-Level GaN Bidirectional Converter with an Active Energy Buffer for Level II Electric Vehicle Charging," 2021 IEEE Applied Power Electronics Conference and Exposition (APEC), Phoenix, AZ, USA, 2021
- [2] Z. Liao, D. Chou, K. Fernandez, Y. -L. Syu and R. C. N. Pilawa-Podgurski, "Architecture and Control of An Interleaved 6-Level Bidirectional Converter With an Active Energy Buffer for Level-II Electric Vehicle Charging," 2020 IEEE Energy Conversion Congress and Exposition (ECCE),
- [3] K. Fernandez et al., "A Bidirectional Liquid-Cooled GaN-based AC/DC Flying Capacitor Multi-Level Converter with Integrated Startup and Additively Manufactured Cold-Plate for Electric Vehicle Charging," 2022 IEEE Applied Power Electronics Conference and Exposition (APEC), Houston, TX, USA, 2022

An EMI-Compliant and Automotive-Rated 48 V-to-PoL Dickson-Based Hybrid Switched Capacitor DC-DC Converter



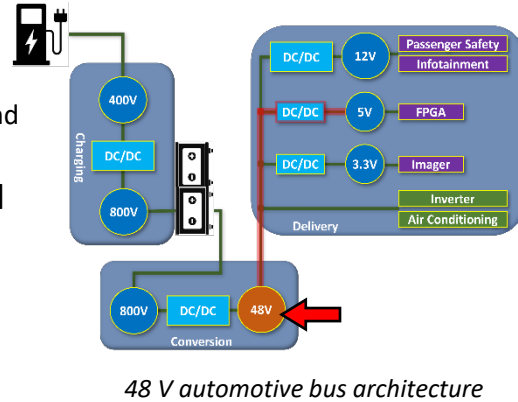
Motivation and Application

Data center power delivery and automotive powertrains tending towards a 48 V distribution rail

- Higher intermediate bus voltages minimize losses and reduce cabling weight

This work demonstrates the merit of hybrid SC topologies for use in 48 V automotive systems

- Regulating Dickson-based hybrid SC topology
- EMI mitigation techniques – filtering and spread-spectrum frequency modulation

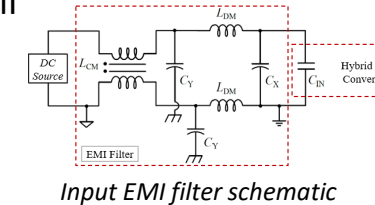


Hardware Implementation

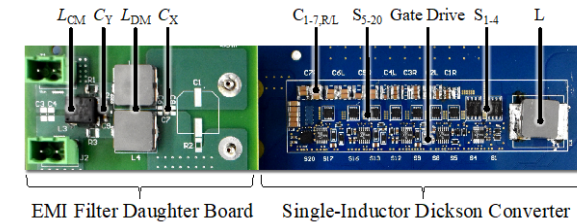
Uses only automotive-qualified parts

Switch selection based on required function, both Si and GaN

EMI input filter and spread spectrum frequency modulation (SSFM) to reduce EMI



Switches and Key Parameters			
Switch	S1-S4	S5-S18	S19-S20
Tech	Si	Si	GaN
Function	Bridge switches	'String' switches	Input switches
$R_{DS(on)}$	1.4 m Ω	3.5 m Ω	2.5 m Ω
V_{DS}	40 V	40 V	80 V



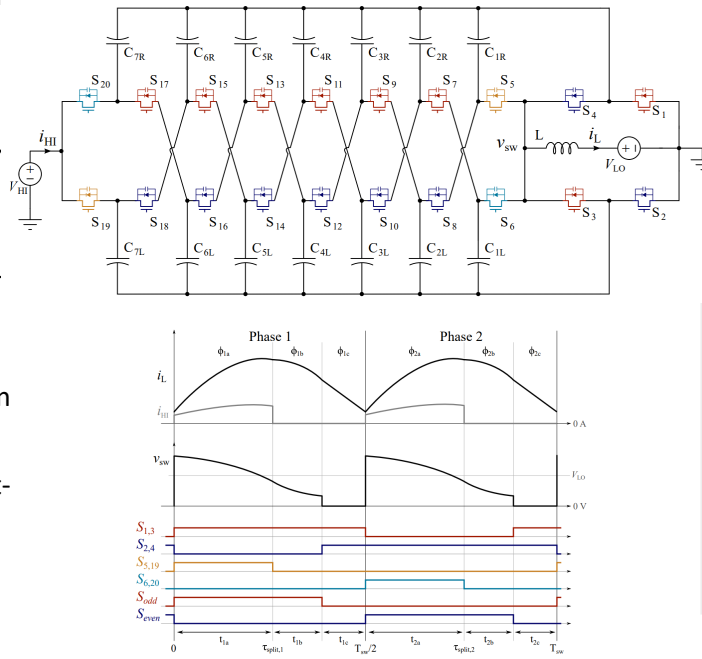
Topology and Challenges

Hybrid switched-capacitor, 8-to-1 interleaved-input, single-inductor Dickson converter

- Differential input \rightarrow continuous input current \rightarrow reduced required input filter
- Inductor at output \rightarrow filtering and EMI shielding at low side
- Inductor at output \rightarrow voltage regulation

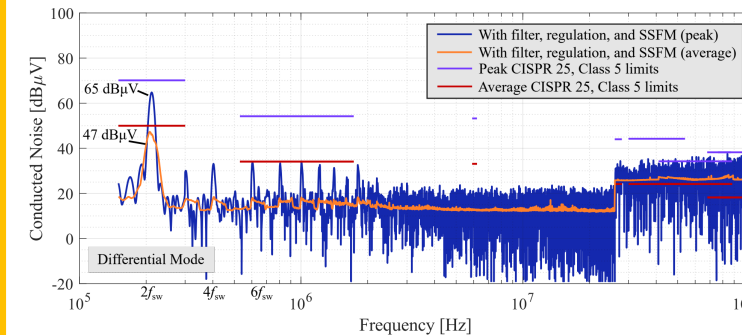
Challenges

- Split-phase switching necessary for soft-charging of the flying capacitors
- Automotive component selection
- High efficiency, power density, and CISPR 25 Class 5 EMI compliance



Experimental Results

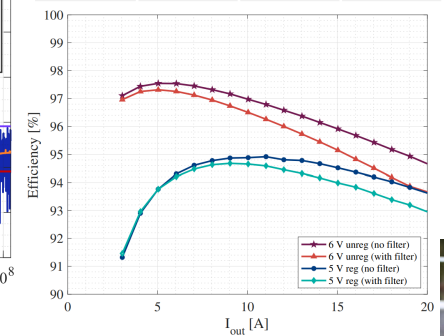
Differential Mode (DM) EMI results



References: [1] M. E. Blackwell, et al., "Direct 48 V to 6 V Automotive Hybrid Switched-Capacitor Converter with Reduced Conducted EMI," 2022 IEEE 23rd Workshop on Control and Modeling for Power Electronics (COMPEL). [2] S. Krishnan, et al., "An EMI-Compliant and Automotive-Rated 48V to Point-of-Load Dickson-Based Hybrid Switched-Capacitor DC-DC Converter," 2023 IEEE Transportation Electrification Conference & Expo (ITEC)

Converter Operating Parameters

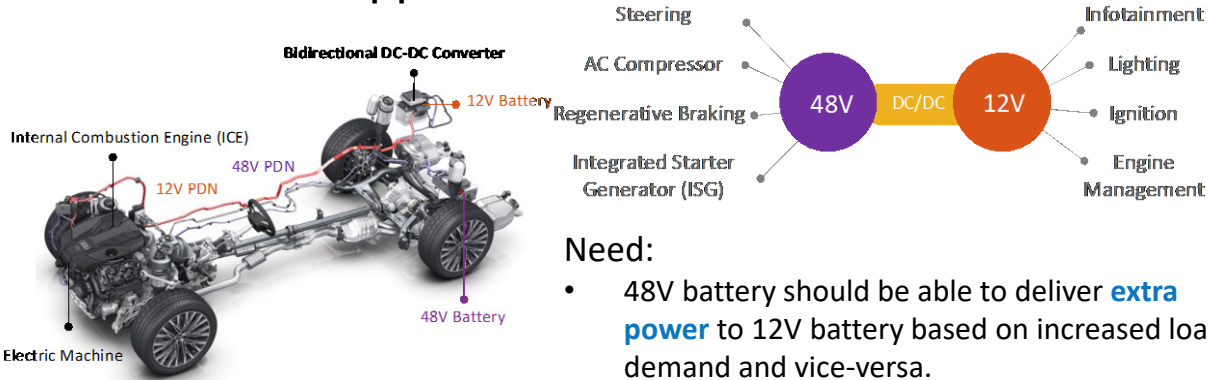
V_{IN}	V_{OUT}	$P_{LO,max}$	f_{sw}
48 V	6 V, 5 V	120 W	106 kHz



Bidirectional Power Transfer in Hybrid Switched-Capacitor Converter for 48V/12V Regulated Automotive Applications



Motivation and Application



Need:

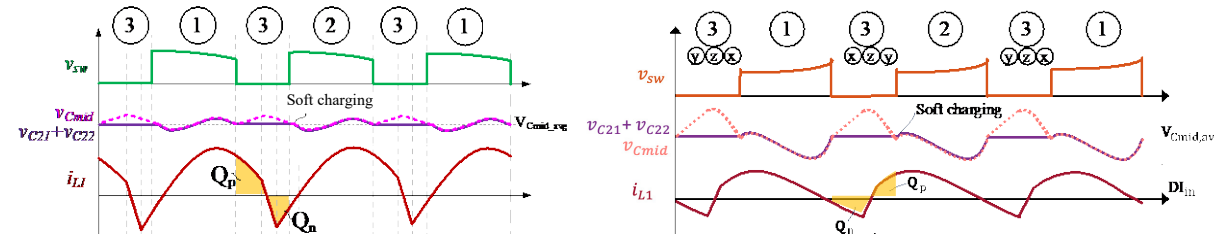
- 48V battery should be able to deliver **extra power** to 12V battery based on increased load demand and vice-versa.

Challenges:

- Delivery of **high current** with **high efficiency** and **high power density in both directions**

Dual Battery System in Mild Hybrid Electric Vehicle (MHEV)
(Source: Audi A8 Powertrain)

Advantages of Proposed Control Technique



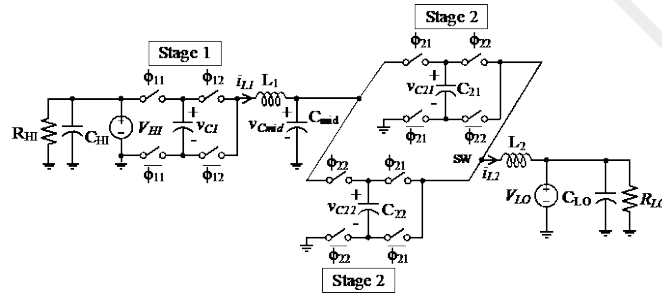
48V to 12V Conversion

12V to 48V Conversion

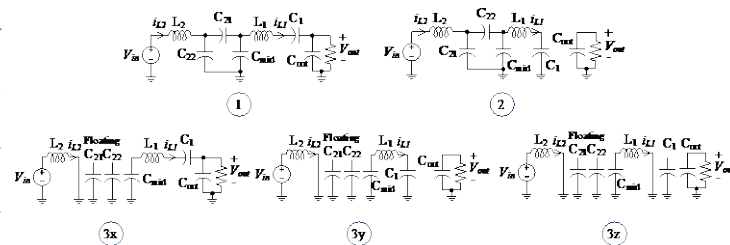
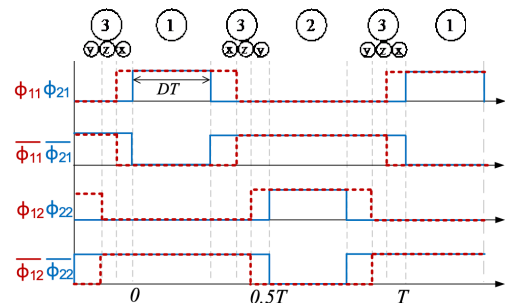
- Implements Natural Balancing of all flying capacitors.
- Achieves Soft-charging and soft-switching.
- Minimizes the size of the intermediate capacitor C_{mid} .

Converter Topology

- 48V-to-12V **regulated** cascaded hybrid resonant-PWM converter [1]
- 1st stage uses a conventional doubler in resonant mode
- 2nd stage used two interleaved doublers operating in PWM mode.

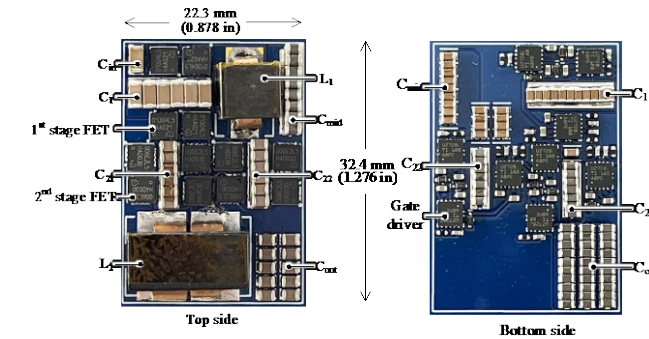
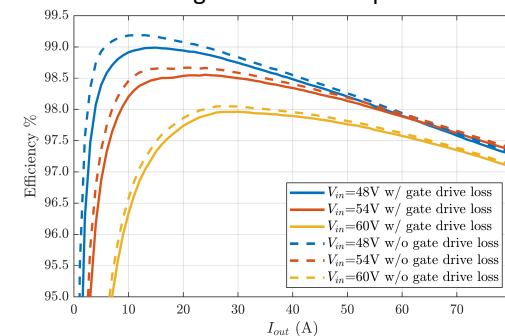


Resonant (Stage-1) + PWM (Stage-2) Operation



Hardware Demonstration and Results

- Measured Efficiency at:
- Input voltage: 48 – 60V
 - 80 A full-load current
 - Regulated 12 V output



- 80A, 99% peak eff. 3115 W/in³ power density
- 21% loss and 63% size reduction over SOTA

[1] T. Ge, et. al., "A Regulated Cascaded Hybrid Switched-Capacitor Converter with Soft-Charging and Zero Voltage Switching for 48-to-12-V," 2023 IEEE APEC.

Nagesh Patle, Ting Ge
Email: {nageshpatle, gting}@berkeley.edu



A General Approach for Design Optimization of High-Performance Hybrid Switched-Capacitor Converters



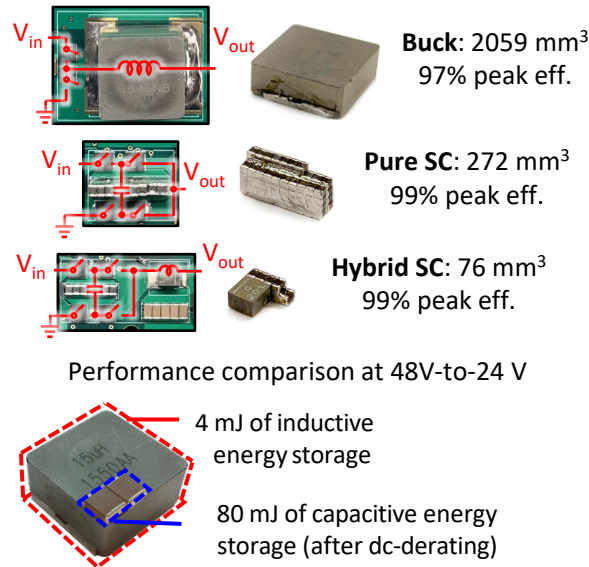
Motivation and Application

Hybrid switched-capacitor converters

- More capacitive energy storage than inductive energy storage for size reduction
- Multiple low-voltage switches in place of a single high-voltage switch for efficiency improvement

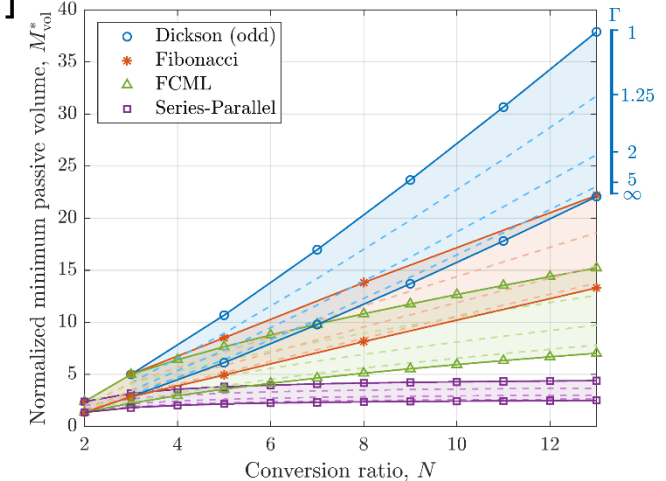
Topology Comparison

- Analytical method to compare relative size and performance of various topologies
- Include the impacts of capacitor voltage ripple and inductor current ripple on passive component volume and switch stress



Impacts of Switching Frequency and Conversion Ratio on Minimal Passive Volume [1]

- Series-Parallel has smaller passive volume → Higher power density
- Increasing $\Gamma = \frac{f_{sw}}{f_{res}} \rightarrow$ smaller passive volume → Higher power density



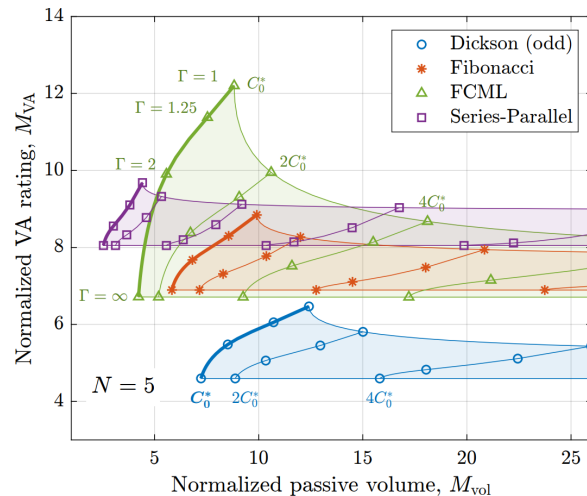
Passive Component Volume and Switch Stress Trade-Off

Increasing the switching frequency beyond resonance

- Trading \uparrow switching loss for \downarrow conduction loss

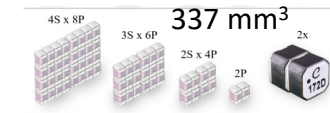
Increasing capacitance beyond minimal volume

- Trading \uparrow volume for \downarrow VA rating (efficiency)

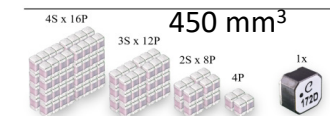


Validation of Analytical Model

Case 1



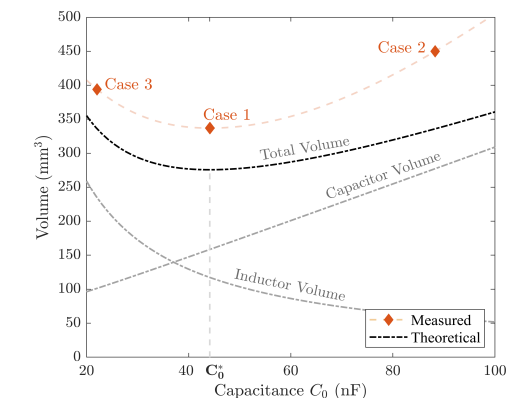
Case 2



Case 3



$$\rho_C = 8800 \text{ J/m}^3 \quad \rho_L = 123 \text{ J/m}^3$$



Passive component volume for varied capacitance to validate minimal volume method



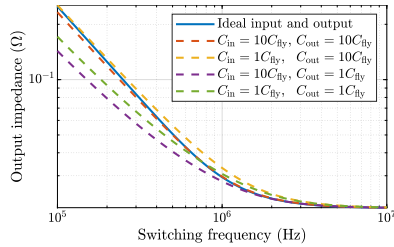
References:

- [1] N. M. Ellis, et. al., "A General Analysis of Resonant Switched Capacitor Converters Using Peak Energy Storage and Switch Stress Including Ripple," in *IEEE Transactions on Power Electronics, Early Access*.
- [2] J. Azurza Anderson, G. Zulauf, J. W. Kolar and G. Deboy, "New Figure-of-Merit Combining Semiconductor and Multi-Level Converter Properties," *OJPEL* 2020.

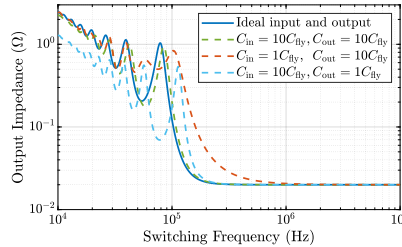
Dr. Nathan Ellis, Maggie Blackwell, Rose Abramson, Dr. Nathan Brooks*, Dr. Sam Coday*
Email: {nathanmilesellis, blackwell, rose_abramson}@berkeley.edu

Background and Motivation

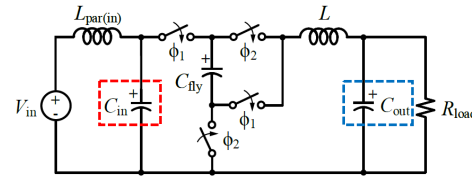
- Insufficient terminal capacitances can greatly affect converter efficiency
- Bulky terminal capacitors become the bottleneck of converter miniaturization



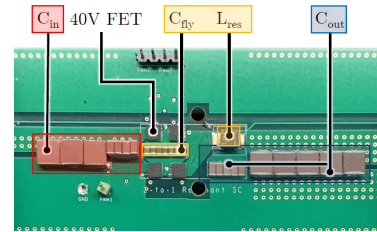
Output impedance of a 2-to-1 pure SC converter with different C_{in} and C_{out}



Output impedance of a 2-to-1 resonant SC converter with different C_{in} and C_{out}



(a) Schematic



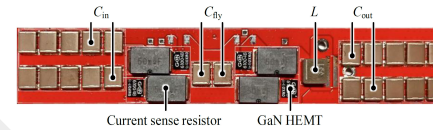
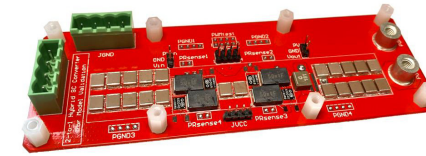
(b) Hardware prototype 2-to-1 resonant SC (ReSC) converter

Simulation and Experimental Verification

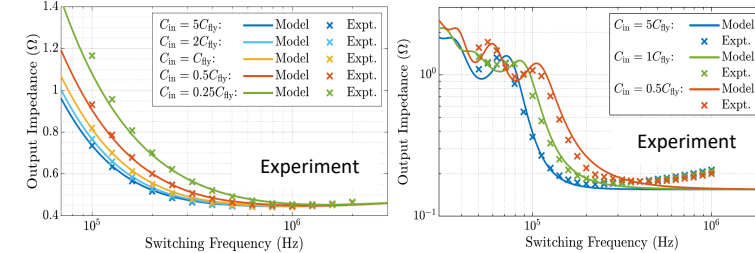
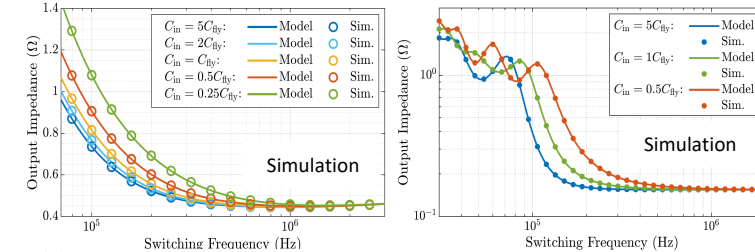
Key considerations

- Minimize switching loss
- Accurate parameter acquisition

High accuracy

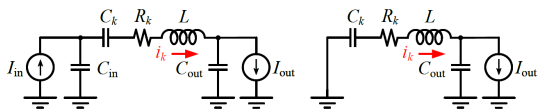


Hardware prototype



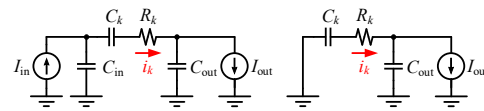
Modeling Derivation and Effect Analysis

Simplified circuit model and general output impedance model



(a) Phase 1 (b) Phase 2

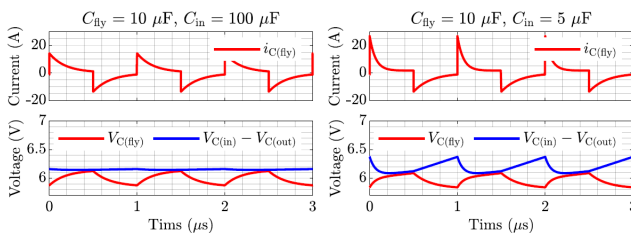
Circuit model of a ReSC converter with C_{in} and C_{out}



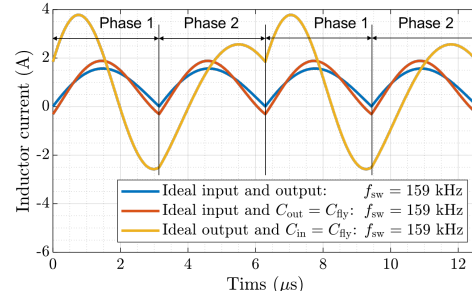
(a) Phase 1 (b) Phase 2

Circuit model of a pure SC converter with C_{in} and C_{out}

Effect of terminal capacitances



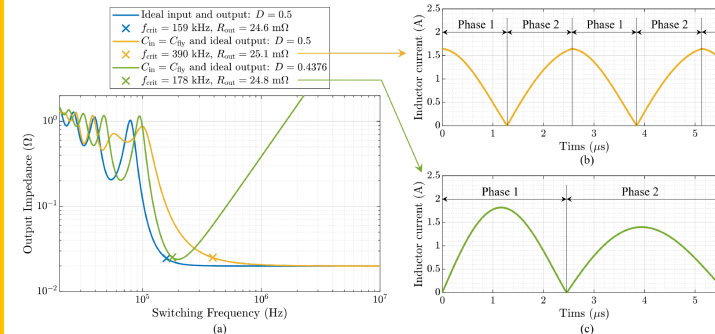
Inductor current waveform of a 2-to-1 pure SC converter with different terminal capacitances



Inductor current waveform of a 2-to-1 ReSC converter with different terminal capacitances

Multi-Resonant Compensation Control (MRCC)

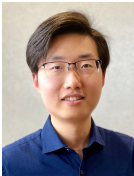
- Challenge: zero current switching (ZCS) is not achievable with 0.5 duty ratio with small C_{in}
- Solution: ensure ZCS operation with the optimal duty ratio and switching frequency
- Result: 5x terminal capacitance reduction without harming efficiency



(a) Comparison of output impedance. (b) Inductor current waveform of the conventional control. (c) Inductor current waveform of MRCC.

References:

- [1] Y. Zhu *et al.*, "Modeling and Analysis of Resonant Switched-Capacitor Converters with Finite Terminal Capacitances," COMPEL 2021.
- [2] Y. Zhu *et al.*, "Multi-Resonant Compensation Control for Terminal Capacitance Reduction in Resonant Switched-Capacitor Converters," COMPEL 2021.
- [3] Y. Zhu *et al.*, "Modeling and Analysis of Switched-Capacitor Converters with Finite Terminal Capacitances," APEC 2021.

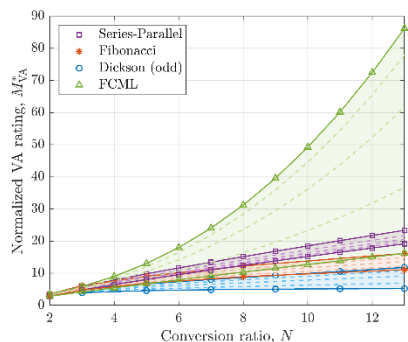


Analysis of Phase Timings for a Zero-Voltage Switching, Split-Phase Hybrid Dickson Converter



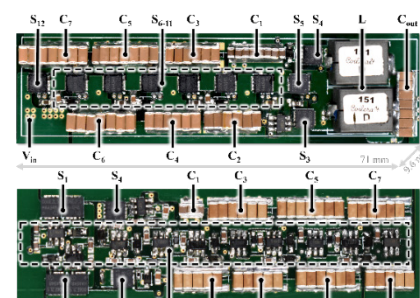
Motivation and Application

- Dickson-based converters are popular for hybrid switched capacitor (SC) solutions due to the reduced switch stress as compared to other topologies [1]
- Applications: high-conversion ratio systems
 - 48 V bus architectures for data centers and automotive powertrains
- Transistor switching losses can be significant share of overall losses, especially with trends towards faster switching frequencies
- Soft-switching techniques, such as zero-current and zero-voltage switching (ZCS and ZVS) can be used to reduce these losses



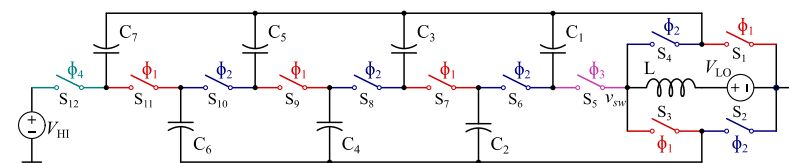
Switch Stress Metric (VA rating) for various hybrid SC converters over conversion ratios showing the Dickson converter having very low relative switch stress

Hardware

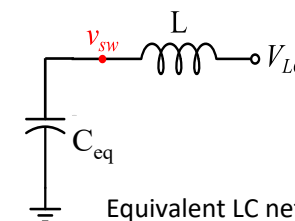


48 V-to-6 V prototype

- Per-phase analysis of an equivalent LC network to determine phase-timings
- Equivalent capacitance C_{eq} :
 - Main phases: A network of the flying capacitors C_1-C_7
 - ZVS sub-phases: A network of linearized transistor output capacitances [2]



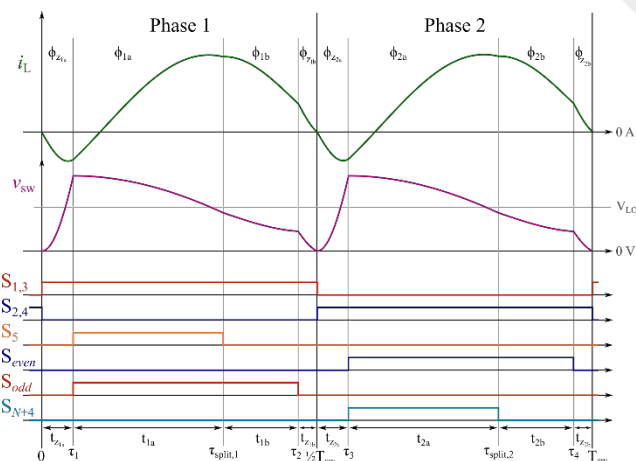
Schematic drawing of the 8-to-1 hybrid Dickson power stage



Equivalent LC network for per-phase analysis

Challenges

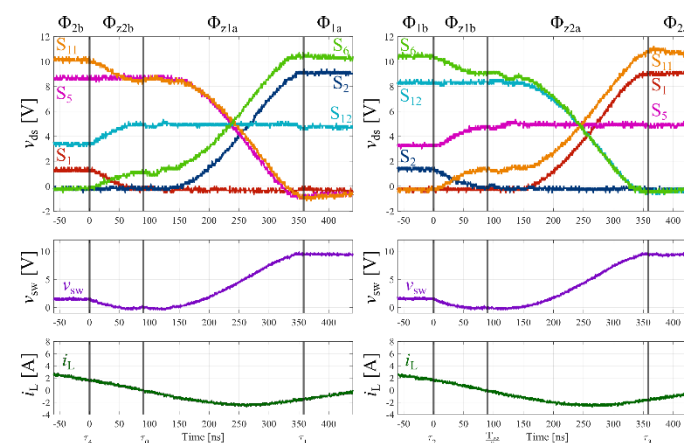
- Phase-timings become non-trivial to determine
- ZVS timings are also non-trivial
 - Non-linear switch output capacitance
 - Multiple switches with different blocking voltages



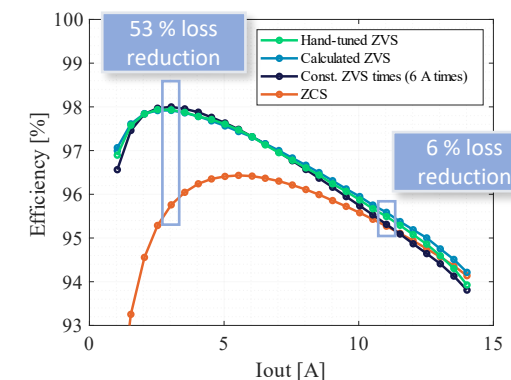
Exemplary phase-timings and waveforms of a resonant Dickson converter achieving ZVS on all switches

References:
 [1] N. M. Ellis, et. al., "A General Approach to Optimization and Control of Resonant Switched Capacitor Converters Using Peak Energy Storage and Switch Stress Including Ripple Considerations," *IEEE Transactions on Power Electronics, Early Access*.
 [2] M. Kasper, R. M. Burkart, G. Deboy, and J. W. Kolar, "ZVS of Power MOSFETs Revisited," *IEEE Transactions on Power Electronics*, vol. 31, no. 12, pp. 8063–8067, Dec 2016.

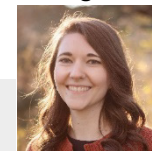
Experimental Verification



Measured drain-source voltages showing ZVS for all switches



An efficiency comparison of ZVS to ZCS, as well as calculated timings to fixed timings

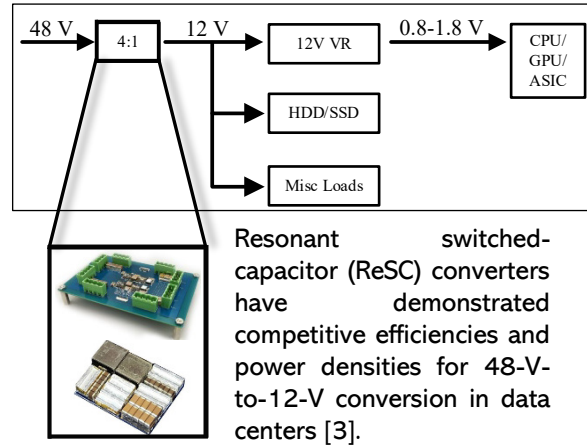


Autotuning of Resonant Switched-Capacitor Converters for Soft Switching Operation



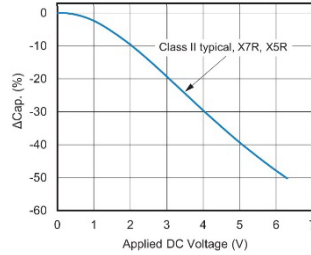
Motivation and Application

Data Center Two-Stage Power Architecture

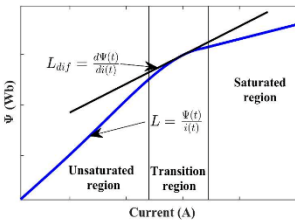


Due to finite terminal filtering capacitances, the efficiency of ReSC converters is often maximized when they are precisely soft switched [4]. However, circuit non idealities render ZCS and ZVS timing challenging to estimate creating the need for active control techniques.

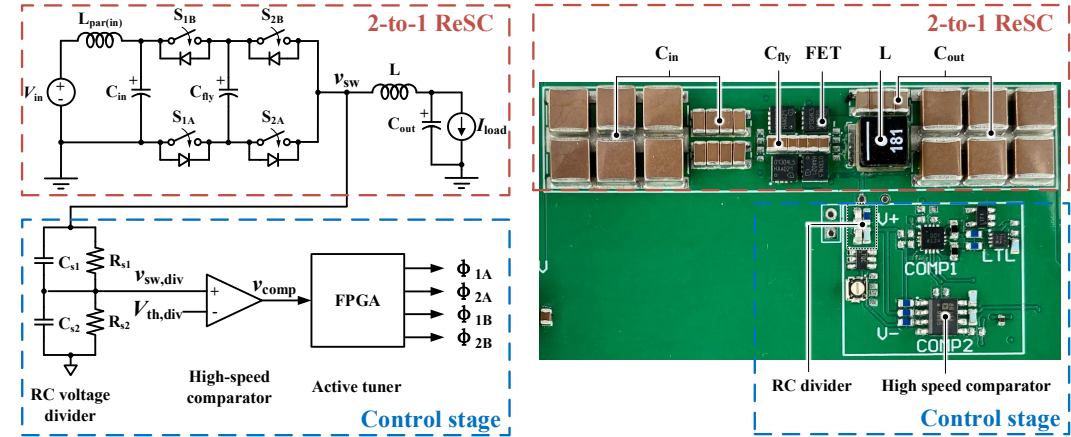
Class II MLCC DC Bias Derating



Inductor Soft Saturation



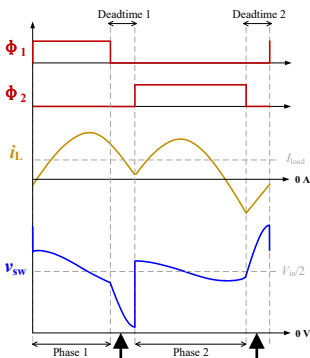
Hardware



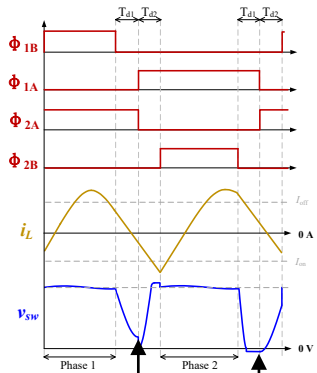
The presented 2-to-1 converter is the foundational ReSC topology. The control technique is verified on a 48-V-to-24-V hardware prototype and can be extended to higher conversion ratio topologies.

Theory and Control

Non-Ideal ZCS

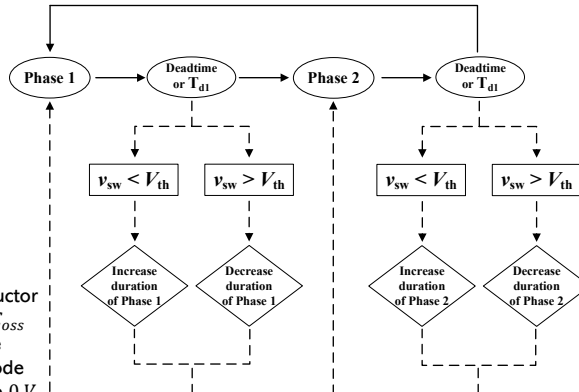


Non-Ideal ZVS



By sensing the switch node voltage, non-ideal soft switching conditions can be detected. Complete ZCS or ZVS can then be achieved by implementing the proposed control scheme.

Control Flowchart

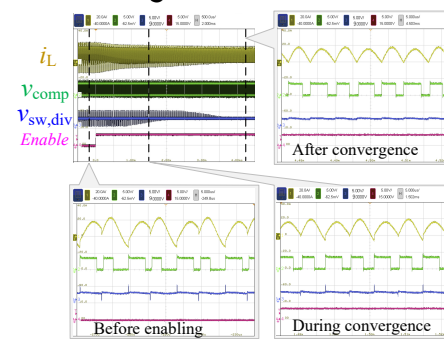


- Positive turn-off inductor current → switch node voltage below $\frac{V_{in}}{2}$
- Negative turn-off inductor current → switch node voltage above $\frac{V_{in}}{2}$
- Insufficient inductor current for C_{oss} discharge → switch node voltage above 0 V
- Excessive inductor current for C_{oss} discharge → switch node voltage above 0 V

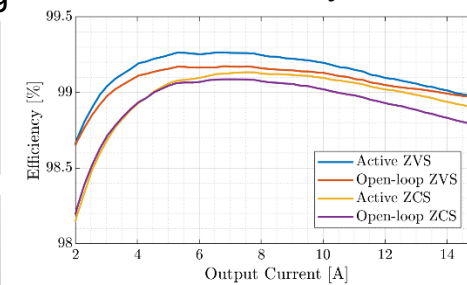
Experimental Verification

- Convergence to complete soft switching can be achieved from a wide range of initial switching frequencies.
- Active ZVS and ZCS control allow for higher peak efficiencies than the conventional open-loop techniques.

Convergence to Soft Switching

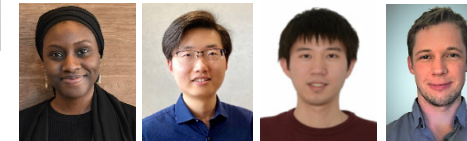


Efficiency



References:

- [1] H. Sambo, Y. Zhu, T. Ge, N. Ellis, and R. Pilawa-Podgurski, "Autotuning of Resonant Switched-Capacitor Converters for Zero Current Switching and Terminal Capacitance Reduction," APEC 2023.
- [2] H. Sambo, Y. Zhu, and R. Pilawa-Podgurski, "Autotuning of Resonant Switched-Capacitor Converters for Zero Voltage Switching," COMPEL 2023.
- [3] T. Ge, Z. Ye, and R. Pilawa-Podgurski, "Geometrical State-Plane Analysis of Resonant Switched-Capacitor Converters: Demonstration on the Cascaded Multiresonant Converter," TPEL 2023.
- [4] Y. Zhu, Z. Ye, T. Ge and R. Pilawa-Podgurski, "Multi-Resonant Compensation Control for Terminal Capacitance Reduction in Resonant Switched-Capacitor Converters," COMPEL 2021.



Students: Haifan Sambo, hsambo@berkeley.edu; Yicheng Zhu yezhu@berkeley.edu; Post-docs: Ting Ge, gting@berkeley.edu; Nathan Miles Ellis, nathanmilesellis@berkeley.edu

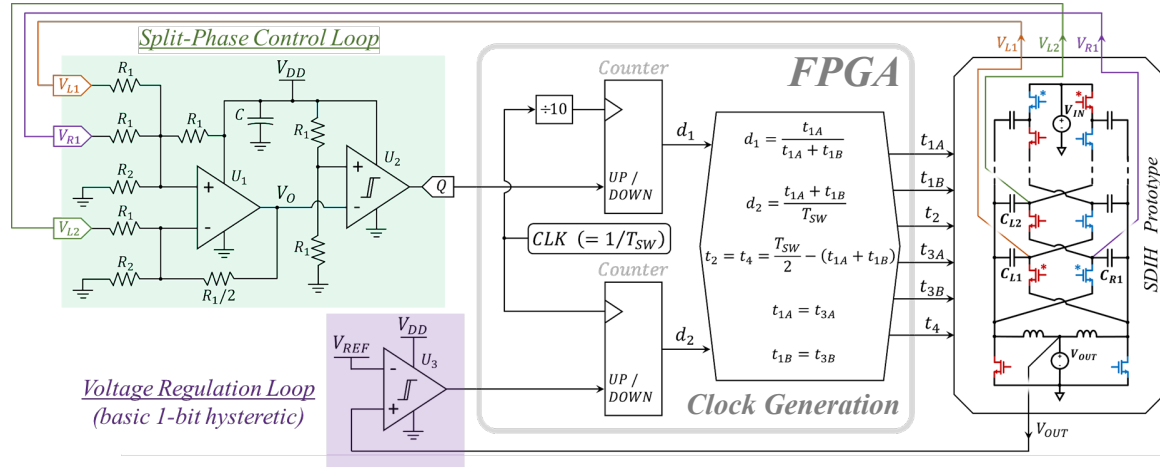
Closed-Loop Split-Phase Control Applied to a Regulating Point-of-Load (PoL) Dickson-Type Converter



Motivation and Application

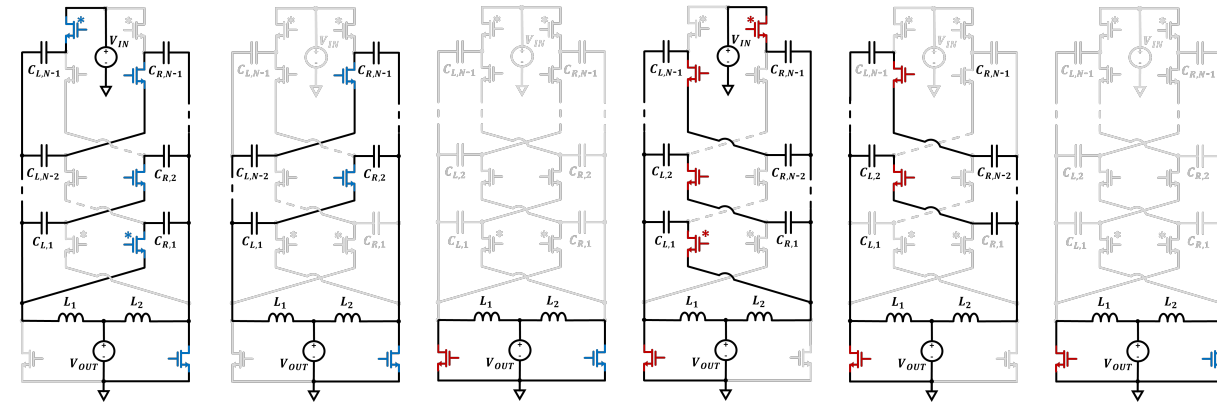
Hybrid Switched Capacitor (HSC) power converter topologies are being adopted in 48V to point-of-load (PoL) applications. Within the HSC converter class, Dickson-type converters [1] achieve the lowest Volt-Amp switch stress, indicative of a smaller semiconductor footprint for equivalent performance. However, some of these topologies require a non-conventional clocking scheme – recently coined as “split-phase switching” [2] – to ensure high efficiency is preserved. Executed in parallel with complimentary work in [3], this work presents a closed-loop split-phase control appropriate for regulating PoL converters [4]; over-coming a key obstacle to the deployment of a new and highly competitive class of hybridized power converter topologies.

Closed-loop Split-phase Control Demonstrated in Hardware



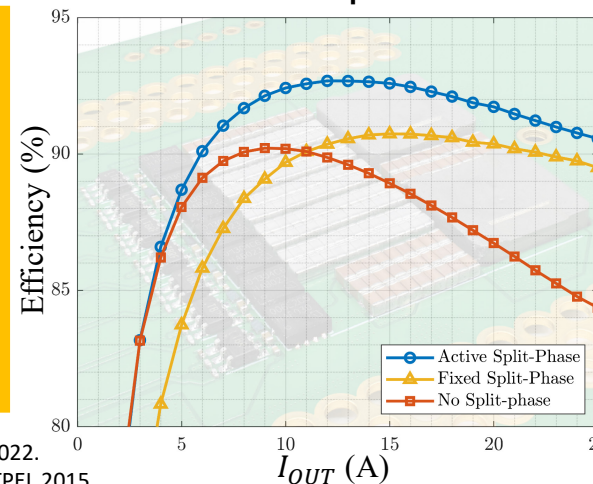
An added Split-Phase Control Loop detects “hard-charging” events and informs appropriate phase timing adjustments within a conventional FPGA-based clock generator.

Example: Phase Progression of the SDIH (Dickson-Type) Converter^[4]



The duration of all phases are fully constrained as a function of V_{IN} , V_{OUT} , I_{IN} , f_{SW} , & component values. The practical inclusion of loss and component derating/mismatch necessitates continuous and dynamic phase duration adjustments.

Experimental Verification



- Closed-Loop Control
- Theoretical Timings
- Without Split-Phase Control

Operating Point	
V_{IN}	48V
V_{OUT}	3.3V
f_{sw}	300 kHz



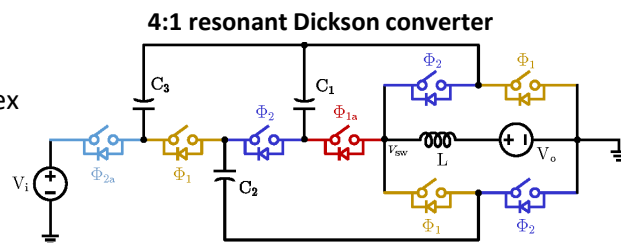
[1] N. Ellis, R. Amirtharajah, “Large Signal Analysis on Variations of the Hybridized Dickson Switched-Capacitor Converter,” TPEL 2022.
 [2] Y. Lei, et. al., “Split-Phase Control: Achieving Complete Soft-Charging Operation of a Dickson Switched-Capacitor Converter,” TPEL 2015.
 [3] R. Abramson, et. al., “An Active Split-Phase Control Technique for Hybrid Switched-Capacitor Converters Using Capacitor Voltage Discontinuity Detection,” COMPEL 2023.
 [4] N. Ellis, et. al., “Closed-Loop Split-Phase Control Applied to the Symmetric Dual Inductor Hybrid (SDIH) Converter,” COMPEL 2023.

Motivation and Application

Dickson-derived converters are increasingly used for both **fixed-ratio** and **direct-to-POL** applications in the datacenter and transportation space. They can achieve **very low switch stress** (i.e. Volt-Amp product), which means that lower-voltage (and therefore less lossy) switches can be used compared to other topologies for a given output power.

Split-Phase Control

Certain Dickson topologies require more complex **split-phase control schemes** [1] in order to achieve full soft-charging of all fly capacitors. Split-phase control timings can be complex to calculate and vary depending on **component tolerance, circuit non-idealities, and operating condition**, necessitating **active control** [2], [3].



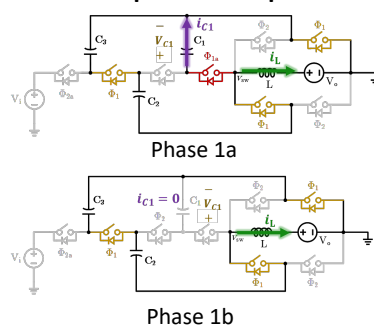
The conventional two-phase operation is split into phases {1a, 1b} and {2a, 2b}

Capacitor Losses: Hard-Charging vs. Soft-Charging

Hard-charging: large charge redistribution loss, spiky currents.

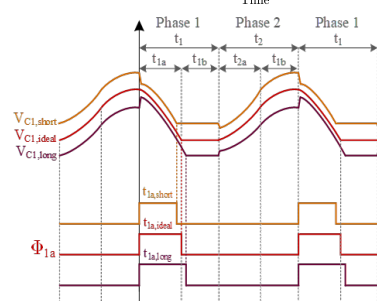
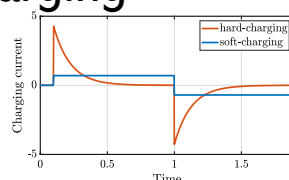
Soft charging: no charge redistribution loss, smooth / resonant currents.

Phase 1 Split-Phase Operation



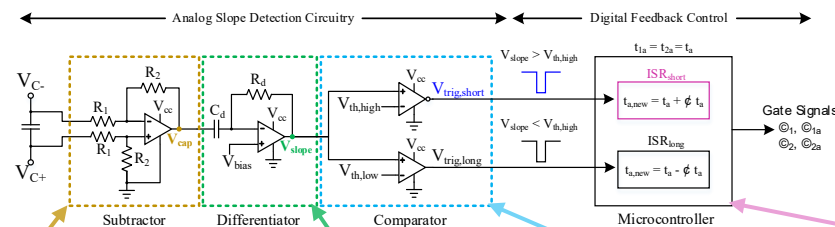
If the {1a,1b} and {2a,2b} transitions occur at the wrong time, hard-charging occurs, resulting in **current spikes** and **discontinuous capacitor voltages**.

These voltage steps can be sensed, allowing the controller to auto-tune split-phase times to achieve soft-charging operation.



References:
 [1] Y. Lei et al., "Split-Phase Control: Achieving Complete Soft-Charging Operation of a Dickson Switched-Capacitor Converter", *IEEE Trans. on Power Electronics*, vol. 31, no. 1, pp. 770-782, 2015. [2] R. A. Abramson et al., "An Active Split-Phase Control Technique for Hybrid Switched-Capacitor Converters Using Capacitor Voltage Discontinuity Detection," *2023 IEEE 24th Workshop on Control and Modeling for Power Electronics (COMPEL)*, Ann Arbor, MI, USA, 2023. [3] N. M. Ellis, H. Sambo and C. N. Robert Pilawa-Podgurski, "Closed-Loop Split-Phase Control Applied to the Symmetric Dual Inductor Hybrid (SDIH) Converter," *2023 IEEE 24th Workshop on Control and Modeling for Power Electronics (COMPEL)*, Ann Arbor, MI, USA, 2023.

Analog Sensing Circuitry



Differential capacitor voltage sensed and signal-conditioned

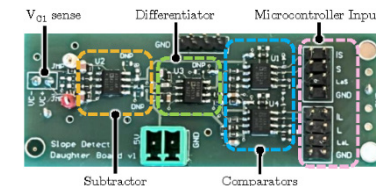
Slope detect circuit triggers on large step discontinuities

Polarity of step discontinuity shows whether split-phase timing is too short or too long

Interrupt service routine (ISR) increases or decreases split-phase timing accordingly

- The analog circuitry is flexible in implementation, and stages can be combined into single package op-amps or off-loaded into internal microcontroller comparator units to increase density.

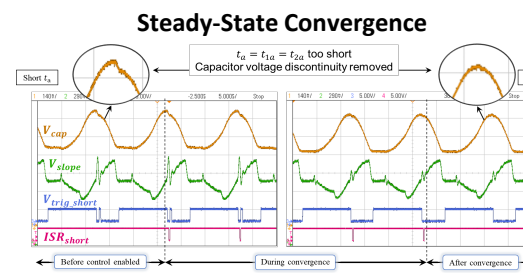
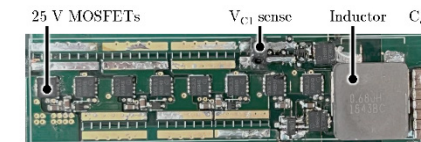
Control Daughterboard



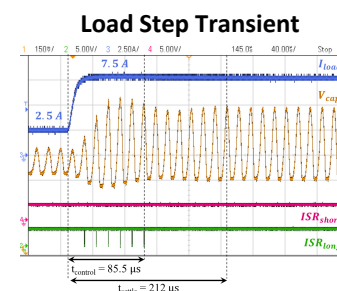
Experimental Verification

- An 8-to-1 resonant Dickson converter was used for validation.
- The control scheme was able to converge on soft-charging split-phase timing when 1) initialized in a hard charging-condition, and 2) when enabled during load step transients.

8:1 Dickson Converter

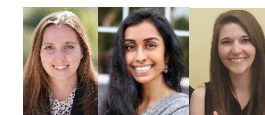


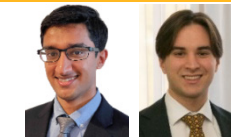
Smooth capacitor voltages signify soft-charging operation



Operating Conditions

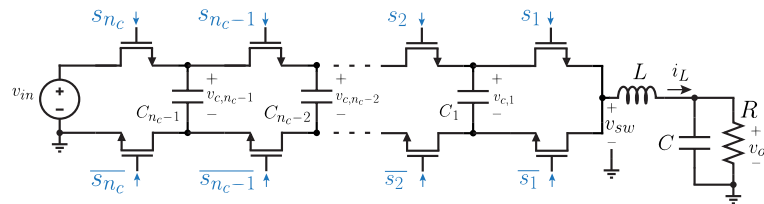
Parameter	Value
V_{in}	48 V
V_{out}	6 V
$I_{out,max}$	10 A



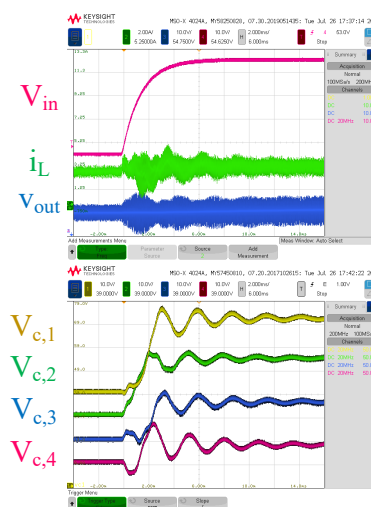


Balancing Control Motivation

- Open-loop balancing of capacitor voltages is unreliable
- Capacitor voltages during large-signal transients exhibit underdamped dynamics
- Peak switch stress may be greater than $\frac{V_{in}}{N-1}$ and can cause switch overvoltage in high-performance designs using low-voltage switches



Natural Balancing

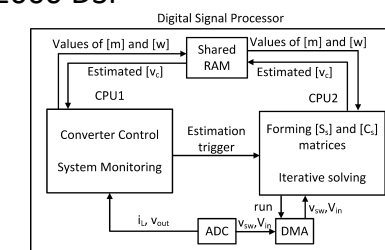


Capacitor Voltage Estimation

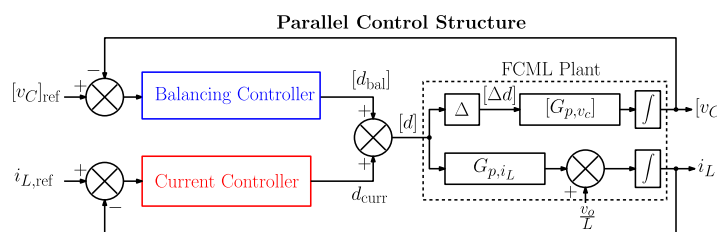
- Active balancing requires measurement of capacitor voltages
- Measuring each capacitor voltage with its own differential sensor is expensive
- Can instead measure switched-node voltage with single-ended sensor and calculate capacitor voltages
- Solve system of equations iteratively with reduced computation burden
- Demonstrated on industry-standard Texas Instruments C2000 DSP

$$\begin{bmatrix} v_{sw}^I \\ v_{sw}^{II} \\ v_{sw}^{III} \\ v_{sw}^{IV} \\ v_{sw}^V \\ v_{sw}^{VI} \end{bmatrix} = \begin{bmatrix} s_1^I & 0 & 0 & 0 & 0 & 0 \\ 0 & s_1^{II} & 0 & 0 & 0 & 0 \\ 0 & 0 & s_1^{III} & 0 & 0 & 0 \\ 0 & 0 & 0 & s_1^{IV} & 0 & 0 \\ 0 & 0 & 0 & 0 & s_1^V & 0 \\ 0 & 0 & 0 & 0 & 0 & s_1^{VI} \end{bmatrix} \begin{bmatrix} V_{in}^I \\ V_{in}^{II} \\ V_{in}^{III} \\ V_{in}^{IV} \\ V_{in}^V \\ V_{in}^{VI} \end{bmatrix} + \begin{bmatrix} s_2^I - s_1^I & s_3^I - s_2^I \\ s_2^{II} - s_1^{II} & s_3^{II} - s_2^{II} \\ s_2^{III} - s_1^{III} & s_3^{III} - s_2^{III} \\ s_2^{IV} - s_1^{IV} & s_3^{IV} - s_2^{IV} \\ s_2^V - s_1^V & s_3^V - s_2^V \\ s_2^{VI} - s_1^{VI} & s_3^{VI} - s_2^{VI} \end{bmatrix} \begin{bmatrix} v_{c1} \\ v_{c2} \end{bmatrix}$$

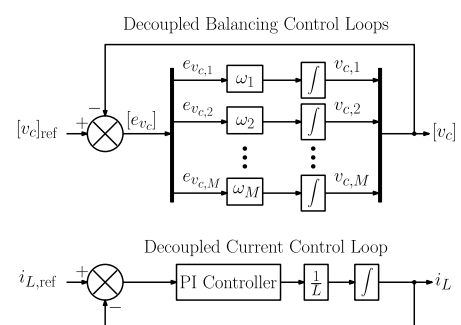
First cell's switch states Capacitor connection matrix



Closed-Loop Control



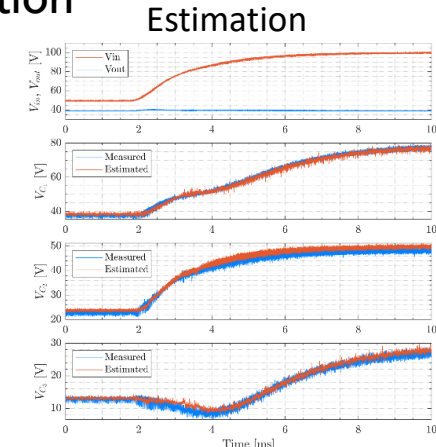
Equivalent Controllers after Decoupling and Feedback Linearization



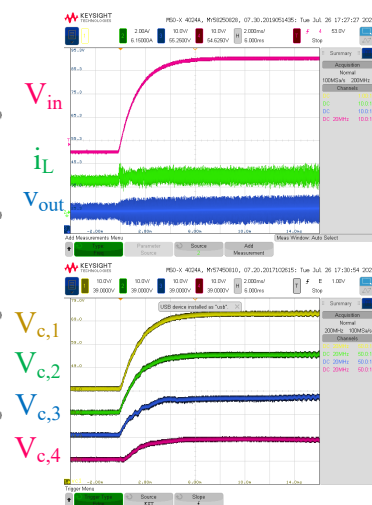
- Model average behavior of FCML converter to obtain "plant" for control
- Structure of plant informs controller design: duty ratios can be controlled differentially to steer capacitor voltages
- Balancing controller runs in parallel with controller(s) regulating load voltage
- Closed-loop system is decoupled – controllers operate without mutual interaction

Experimental Verification

- Active balancing ensures capacitor voltages track nominal values during supply transients
- Single-sensor estimation of capacitor voltages is reliable and low-cost



Active Balancing



References:
 [1] R. K. Iyer, et al., "A High-Bandwidth Parallel Active Balancing Controller for Current-Controlled Flying Capacitor Multilevel Converters," 2023 IEEE Applied Power Electronics Conference and Exposition (APEC).
 [2] I. Z. Petric, et al., "A Real-Time Estimator for Capacitor Voltages in the Flying Capacitor Multilevel Converter," 2022 IEEE 23rd Workshop on Control and Modeling for Power Electronics (COMPEL).

A Hybrid Switched-Capacitor Solar Microinverter Utilizing a Fixed-ratio Resonant DC-DC Stage and Flying Capacitor Multi-level DC-AC Stage

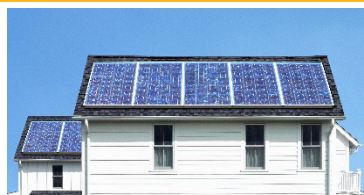


Berkeley Power and Energy Center

Motivation and Application

Hybrid Switched-Capacitor Converters

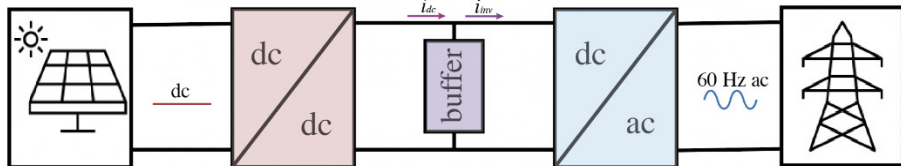
- The Cascaded Series-Parallel converter (CaSP) has been used as a power-dense dc-dc step-down solution in the 48V application space but is being adapted use as a boost stage [1].
- The flying capacitor multilevel converter (FCML) can be used to step down the



Rooftop solar requires **efficient** and **power dense** solutions to convert power for use in homes and at the grid.

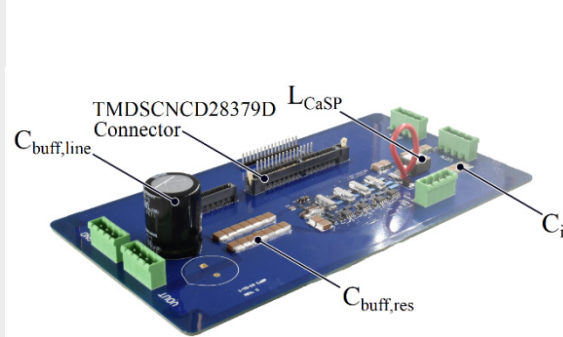


Example inverter: Enphase IQ8



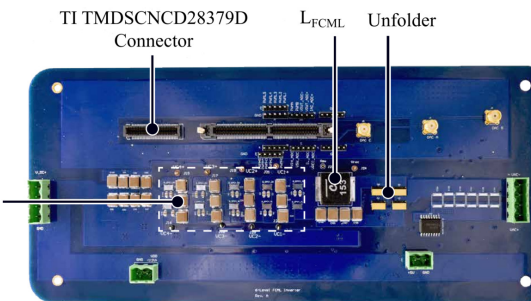
Full microinverter concept.

Hardware



CaSP System Specifications

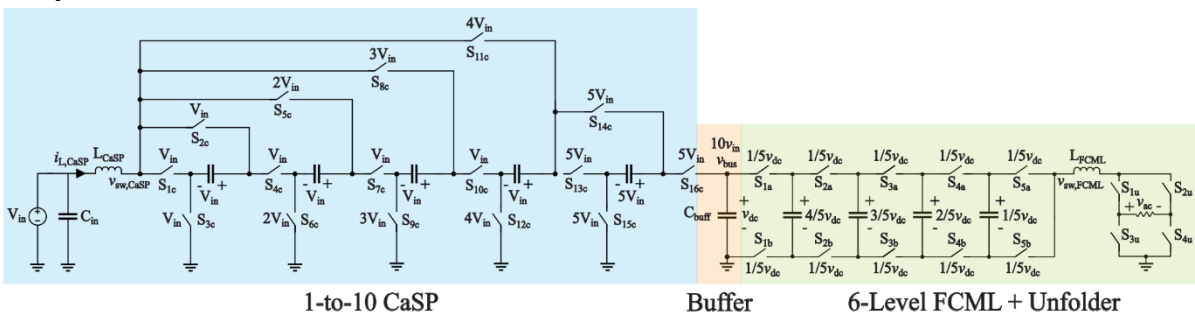
- 35-40V input
- 350-400V, 500W output



FCML System Specifications

- 350-400V input, 500W+
- Sensing for control included on this board.
- 2nd revision coming soon

System Architecture

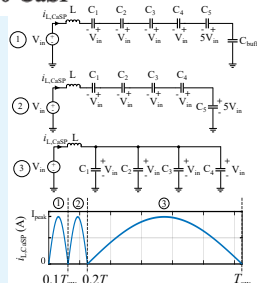


1-to-10 CaSP

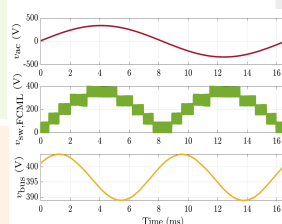
Buffer

6-Level FCML + Unfolder

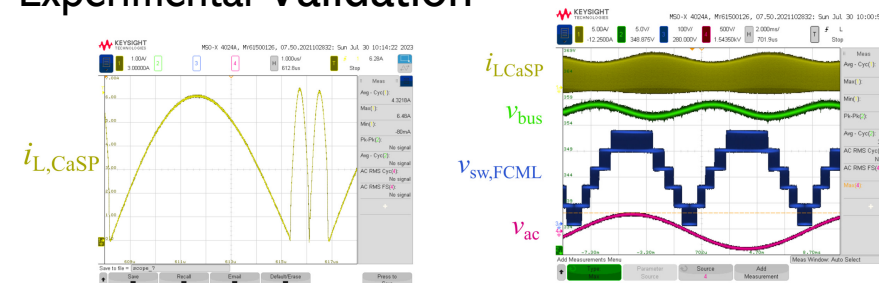
- Three sub-intervals of one switching cycle, each with a unique resonant LC tank impedance [2].
- Achieves ZCS, partial ZVS.
- Can be used as stand-alone startup circuitry.



- 400V to 240Vac. Voltage at output of inductor is rectified sine wave that is unfolded by H-bridge.
- HV buffer allows for reduction of capacitance due to smaller current ripple



Experimental Validation



System waveforms with 240 V_{ac} output

- System able to produce 240 Vac output at light load
- CaSP achieves ZCS during full system operation at 240 Vac output

Peak efficiency with 255 Vac output at light load: **93.5%**

References:

[1] R. A. Abramson, Z. Ye, T. Ge and R. C. N. Pilawa-Podgurski, "A High Performance 48-to-6 V Multi-Resonant Cascaded Series-Parallel (CaSP) Switched-Capacitor Converter," 2021 IEEE Applied Power Electronics Conference and Exposition (APEC), Phoenix, AZ, USA, 2021
 [2] K. Fernandez and R. C. N. Pilawa-Podgurski, "A 1-to-10 Fixed-Ratio Step-up Multi-Resonant Cascaded Series-Parallel (CaSP) Switched-Capacitor Converter with Zero-Current Switching," 2023 11th International Conference on Power Electronics and ECCE Asia (ICPE 2023 - ECCE Asia), 2023

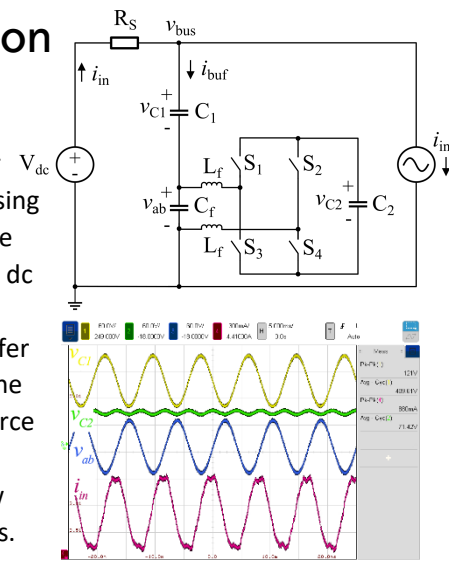


A Charge Injection Loss Compensation Method for a Series-Stacked Buffer to Reduce Current and Voltage Ripple in Single-Phase Systems



Motivation and Application

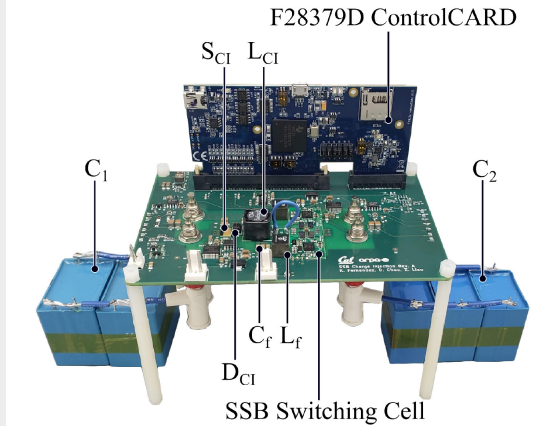
The Series-stacked buffer (SSB) is an active buffer topology that achieves high energy utilization and greatly decreases the power conversion system volume without comprising efficiency [2]. However, there can be a large amount of residual ac current ripple on the dc bus due to SSB's control methodology that injects real power through the reactive buffer branch. This control is required to charge the C_2 capacitor in the SSB that acts as a dc source for a full-bridge converter. Specifically, this ripple gets is worse in applications with low source impedance, such as battery systems.



SSB circuit that handles reactive buffering. Real power is injected to charge C_2 .

The real power injection causes large ac current ripple along the dc-link i_{in} . (24% ac current ripple shown at 1.5 kW at 400 V_{dc}).

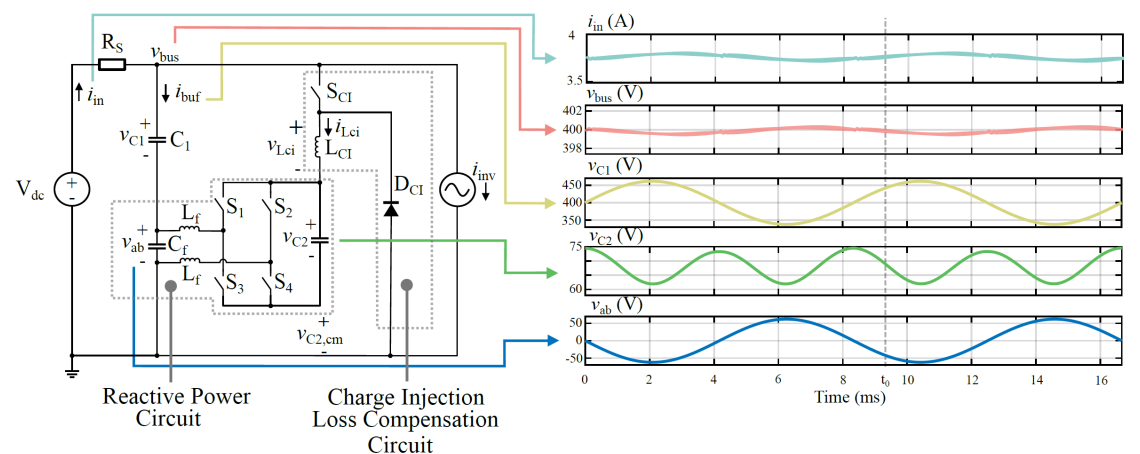
Hardware



Component	Part No.	Parameters
$S_1 - S_4$	EPC2033	150 V, 6 m Ω
S_{CI}	GaN Systems GS66506T	600 V, 2 A
D_{CI}	ON Semiconductor MURS160T3G	650 V, 67 m Ω
L_{CI}	Coilcraft MSS1210-104	100 μ H
C_1	TDK B32524Q1686K000	100 V, 68 μ F x 3
C_2	TDK B32776G4406K000	450 V, 40 μ F x 2

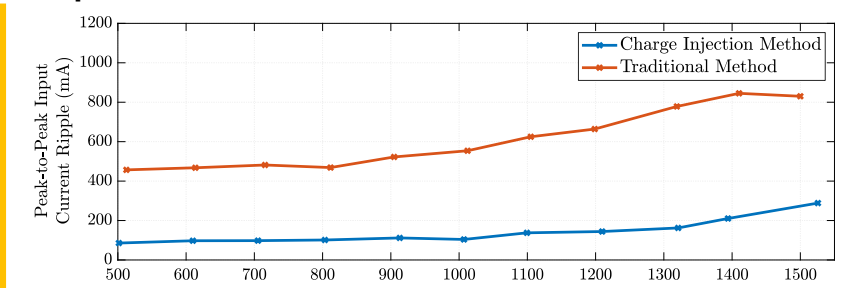
Proof of concept hardware. GaN devices are used for all switches. The volume of this design can be further reduced by using the optimization methodology shown in [3].

Proposed "Charge Injection" Method



The Charge Injection method has a separate branch that handles real power delivery while the rest of the SSB handles the reactive power buffering. As a result, the dc-link current ripple is greatly reduced.

Experimental Verification



The peak-to-peak ac current ripple is reduced:

- By maximum of **5.3x**
- And average of **4.3x**
- **3x** at peak load

Charge Injection method achieves an average **efficiency of 99.4%** across all loads.

References:

[1] K. Fernandez, N. Brooks, T. Ge, Z. Liao, R. C. N. Pilawa-Podgurski, "A Charge Injection Loss Compensation Method for a Series-Stacked Buffer to Reduce Current and Voltage Ripple in Single-Phase Systems" in 2022 Applied Power Electronics Conference (APEC), 2022.

[2] Z. Liao, et al. "A High Power Density Power Factor Correction Converter with a Multilevel Boost Front-End and a Series-Stacked Energy Decoupling Buffer," 2018 IEEE Energy Conversion Congress and Exposition (ECCE), 2018, pp. 7229-7235,

[3] Z. Liao, et al. "Multi-objective optimization of series-stacked energy decoupling buffers in single-phase converters," in 2018 IEEE19th Workshop on Control and Modeling for Power Electronics (COMPEL), July 2018, pp. 1-7.

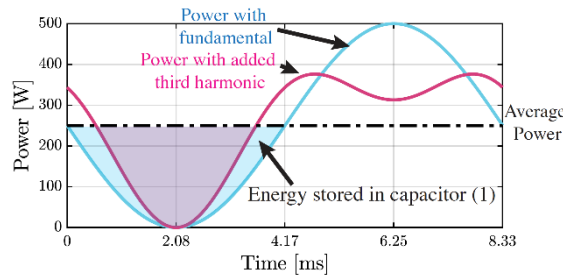


Utilizing Harmonic Injection to Reduce Energy Storage in a Single-Phase Active Energy Buffer



Motivation

- Single-phase power converters rated for high power applications require reactive buffering on the dc bus to maintain a constant and clean dc power input or output. Often this is a bulky electrolytic capacitor.
- [1] found that buffer storage requirements for a passive buffer could be reduced 56% for the addition of allowable 3rd and 5th harmonics
- We apply this harmonic injection method for energy storage reduction in the capacitors of the series-stacked buffer (SSB), which is a power-dense alternative to the conventional capacitor solution.

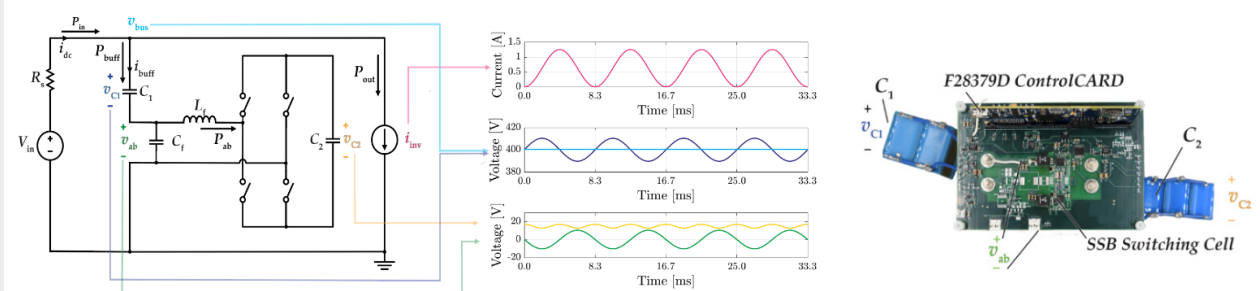


Energy storage in buffer during a twice-line frequency cycle.

$$W_{store} = \int_0^{T/2} P_{buff}(t) dt$$

$$W_{store} = \frac{1}{2} CV_{max}^2 - \frac{1}{2} CV_{min}^2$$

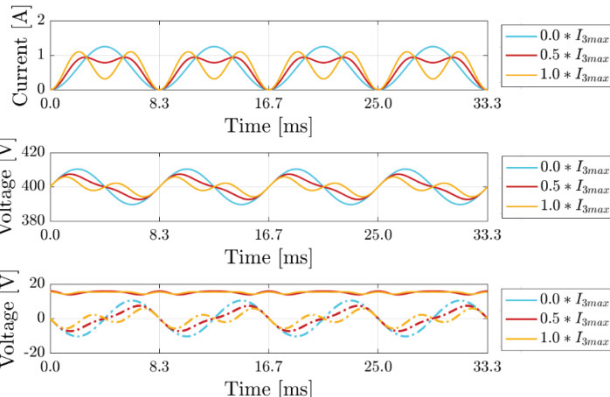
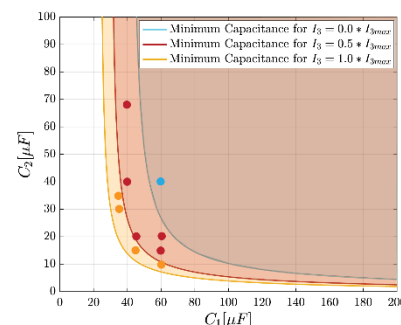
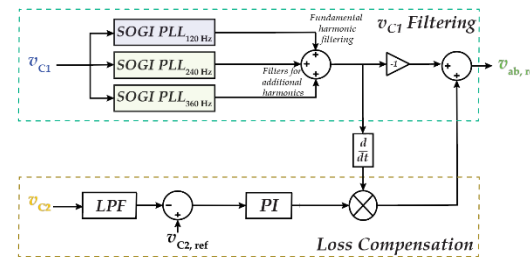
Circuit Topology and Hardware



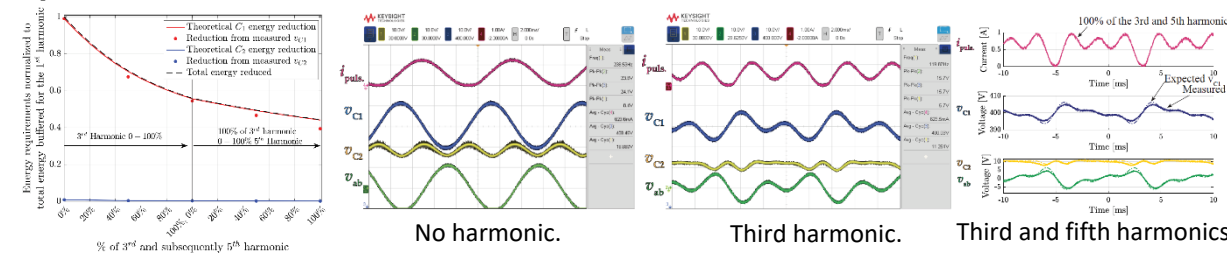
The SSB is an active buffer that combines a primary energy buffer capacitor with an H-bridge. This permits a larger voltage ripple across the main energy storage capacitor maximizing the amount of energy buffered, and subsequently the energy utilization ratio [2].

Challenges and Control

- Determining the expected voltage ripple on each of the capacitors is nontrivial.
- Figure out how to control an active buffer when additional harmonics are added to the system.



Experimental Verification



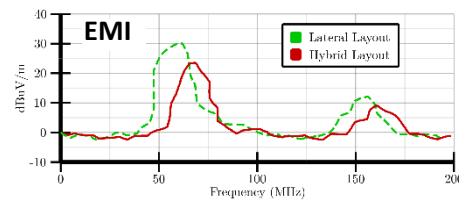
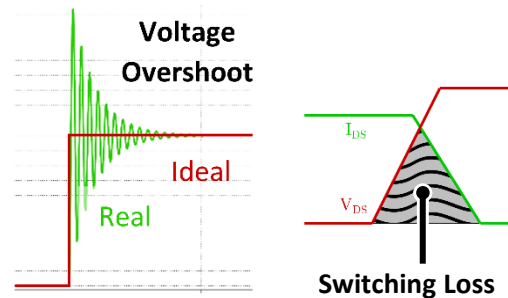
55% reduction in required energy storage split between two capacitors. In an example case, C_1 can be reduced from $60\mu F$ to $34\mu F$, and C_2 from $27\mu F$ to $20\mu F$ for same dc-bus voltage ripple [3].

References:
 [1] A. J. Hanson, A. F. Martin, and D. J. Perreault, "Energy and Size Reduction of Grid-Interfaced Energy Buffers Through Line Waveform Control," *IEEE Transactions on Power Electronics*, Nov. 2019
 [2] N. C. Brooks, S. Qin, and R. C. N. Pilawa-Podgurski, "Design of an active power pulsation buffer using an equivalent series-resonant impedance model," in *2017 IEEE 18th Workshop on Control and Modeling for Power Electronics*, Jul. 2017
 [3] F. Giardine, N. C. Brooks, K. Fernandez and R. C. N. Pilawa-Podgurski, "Utilizing Harmonic Injection to Reduce Energy Storage and Required Capacitance in an Active Series-Stacked Energy Buffer for Single-Phase Systems," *2022 IEEE 23rd Workshop on Control and Modeling for Power Electronics*, 2022



Motivation and Application

Power converters operate by switching between different circuit states. Ideally, the switching transitions would be instantaneous and lossless. In reality, parasitic effects cause switching losses, voltage overshoot, and electromagnetic interference. Advanced design techniques are presented here, which mitigate these effects and enable unprecedented performance.



Interleaved Commutation Loop Layout [2]

Commutation loop inductance is critical to switching performance. Advanced layout techniques can be utilized to reduce this inductance.

Interleaved hybrid decoupling capacitor loops with electrically thin vertical bulk capacitor loop

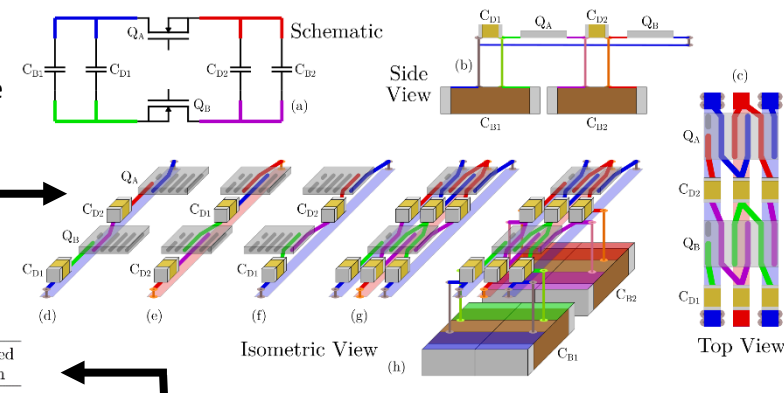
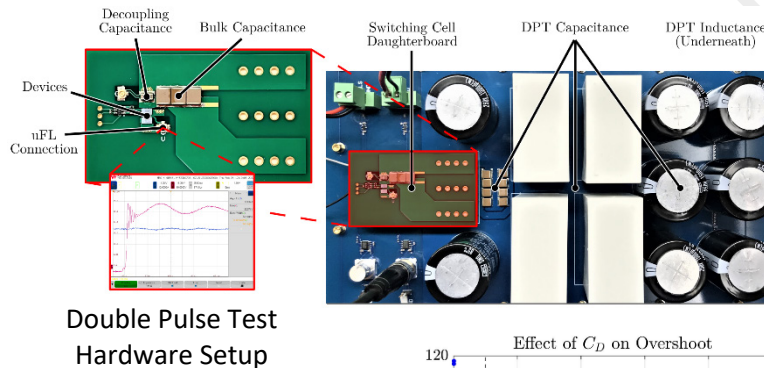
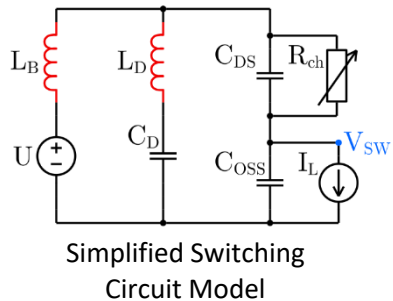


Table 1: Commutation Loop Comparison

Switching Cell Design	Electrically Thin	Hybrid & E-thin	Hybrid Reference	Proposed Design
Simulated Inductance	1.15 nH	450 pH	521 pH	443 pH
Measured Inductance	2.85 nH	940 pH	—	1.14 nH
Board Area	370 mm ²	330 mm ²	420 mm ²	420 mm ²

- Proposed design achieves nearly 3x better performance than best approach without decoupling capacitors
- 20% better than state of the art

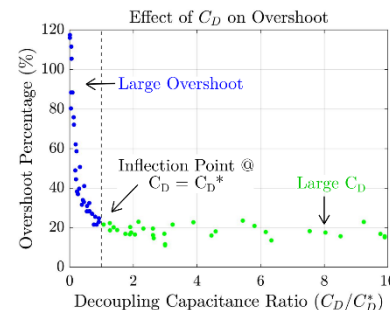
Optimal Decoupling Capacitor Sizing [1]



Determined optimal decoupling capacitor size given load current and output capacitance of the device:

$$C_D^* = 10 * \max\{C_{OSS}, 2L_B I_{ML}^2 / U_{ML}^2\}$$

Experimental Data

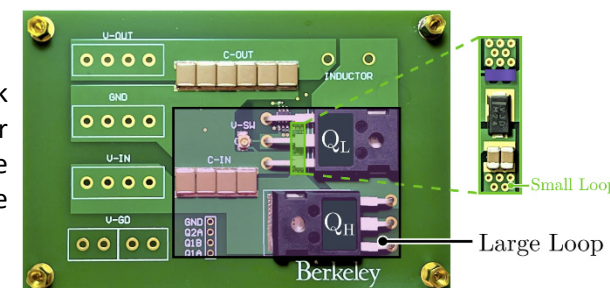


Decoupling Device [3]

For many applications, transistors with large through-hole packages are used, due to their high power handling capability. In this work, a small surface-mount gallium-nitride transistor is added to improve switching performance.

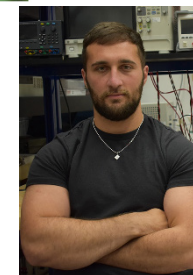
50% reduction in losses

Buck converter hardware prototype



References:

- L. Horowitz and R. C. N. Pilawa-Podgurski, "On Decoupling Capacitor Size in GaN-Based Power Converters," 2022 IEEE 23rd Workshop on Control and Modeling for Power Electronics (COMPEL), Tel Aviv, Israel, 2022, pp. 1-5, doi: 10.1109/COMPEL53829.2022.9830000.
- L. Horowitz and R. C. N. Pilawa-Podgurski, "Modular Switching Cell Design for High-Performance Flying Capacitor Multilevel Converter," 2022 IEEE Applied Power Electronics Conference and Exposition (APEC), Houston, TX, USA, 2022, pp. 342-347, doi: 10.1109/APEC43599.2022.9773604.
- L. Horowitz, N. M. Ellis and R. C. N. Pilawa-Podgurski, "Decoupling Device for Small Commutation Loop and Improved Switching Performance with Large Power Transistors," 2023 IEEE Applied Power Electronics Conference and Exposition (APEC), Orlando, FL, USA, 2023, pp. 2620-2624, doi: 10.1109/APEC43580.2023.10131426.

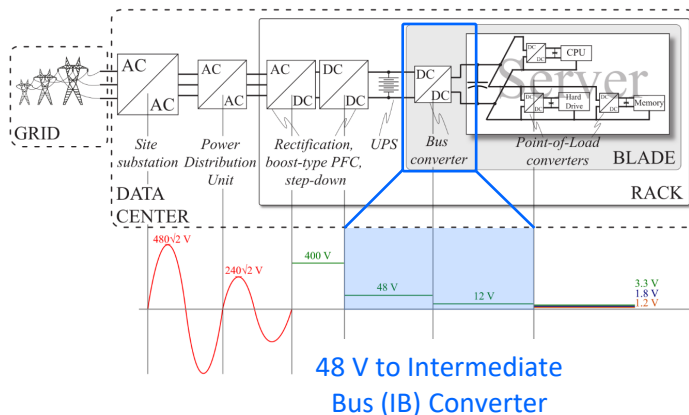


Concluded Research Projects
(with potential follow-up
work in planning stages)

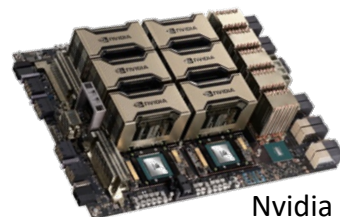


Motivation and Applications

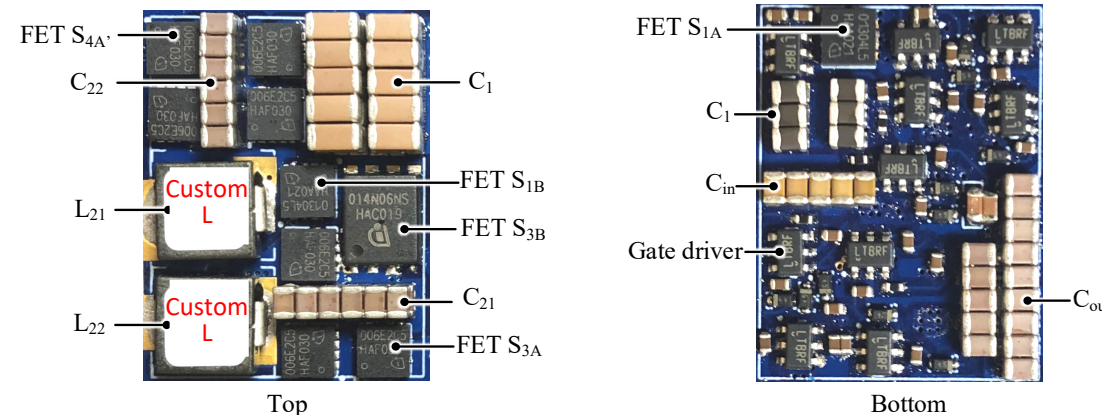
48 V data center power delivery architecture



- The intermediate bus converter in 48 V data center application requires high efficiency and high power density
- Regulation and isolation are not required



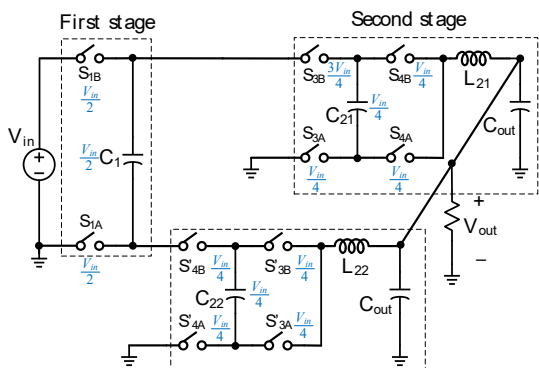
Hardware Demonstration



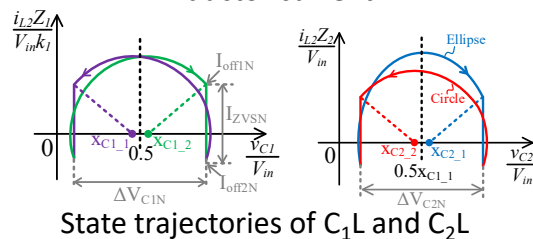
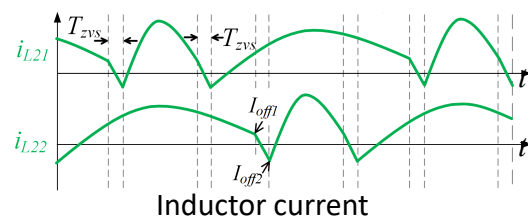
- Dimensions: 17.3 × 23 × 6.6 mm power density: **6000 W/in³** at 12 V output
- 80 A** continuous output and **130 A** - 2 ms transient output

Proposed Topology

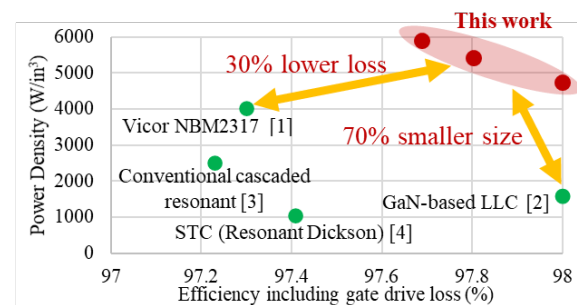
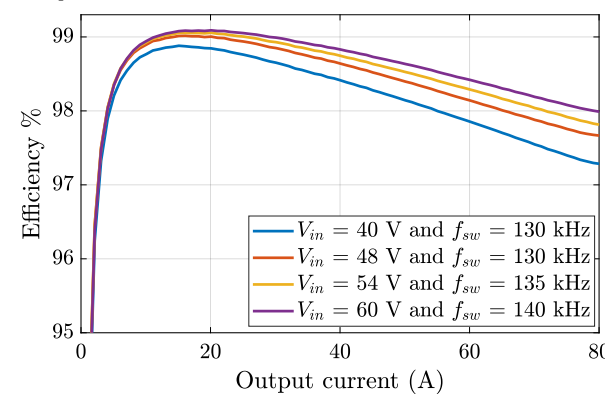
- Cascaded Multi-Resonant converter
- 1st stage uses only two switches to save space of active components, and gate drive level shifters



- State-plane method is used to calculate multi-resonant inductor current



Experimental Results



Comparison with State-of-the-Art 48-to-12 V Solutions

Measured efficiencies including gate drive loss

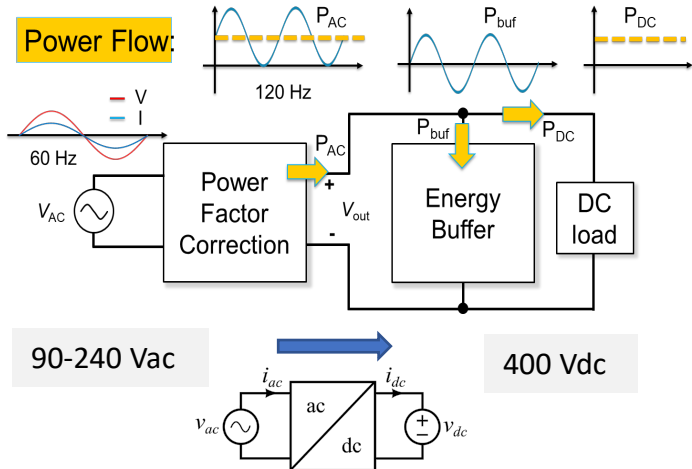
Reference: T. Ge, Z. Ye and R. C. N. Pilawa-Podgurski, "A 48-to-12 V Cascaded Multi-Resonant Switched Capacitor Converter with 4700 W/in³ Power Density and 98.9% Efficiency," 2021 IEEE ECCE.



High Performance Single-phase Ac-dc Conversion with Advanced Topology and Control



Motivation and Application



90-240 Vac to 400 Vdc is a critical conversion stage for applications such as data center power delivery, electric vehicle charging, etc.

Ac-dc power factor correction

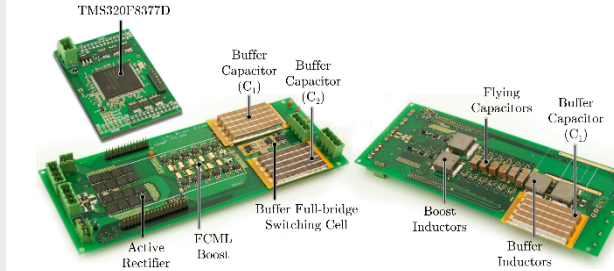
Reduce boost inductor size

Twice-line frequency power ripple buffering

Reduce buffer capacitor size

Hardware Implementation

90-240 Vac to 400 Vdc, 1.5 kW PFC converter [1]

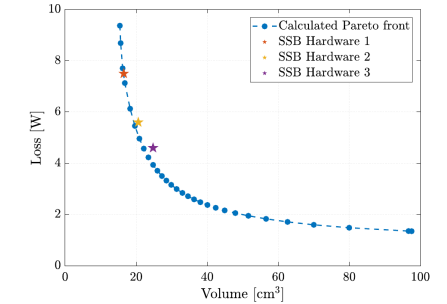


Single DSP TMS320F28377D for the proposed system control

GaN System and EPC GaN FETs used in FCML and SSB for high efficiency

Multi-objective optimization for SSB [2]

Loss-volume Pareto front of SSB generated with numerical optimization method

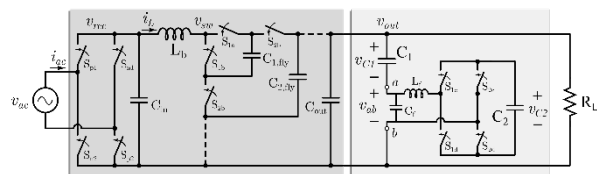


$$\min_{C_1, C_2, V_{C1, dc}} \alpha \cdot \frac{f_{loss}}{F_{loss, max}} + (1 - \alpha) \cdot \frac{f_{volume}}{F_{volume, max}}$$

$$s.t. \quad g_i \leq 0 \quad \forall i = 1, \dots, 4.$$

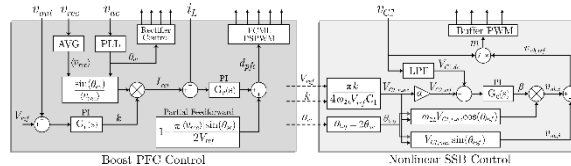
Challenges and Solutions

Topology



- The boost inductor size is reduced flying capacitor multilevel (FCML) topology
- An active buffer topology - series-stacked buffer (SSB) is implemented to reduce the buffer capacitor for twice-line frequency power ripple buffering

Control

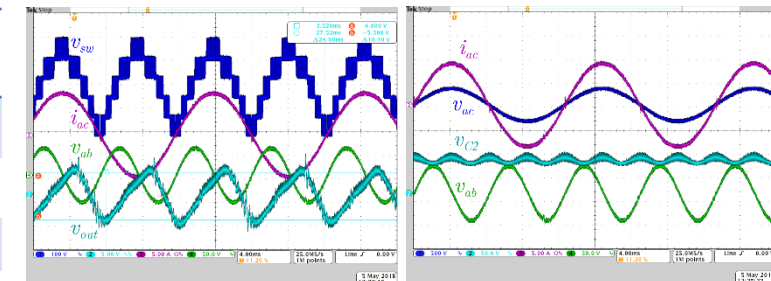


PFC+SSB Coupled Control:

- PFC Multi-loop control:** high-bandwidth "inner" current & low-bandwidth "outer" voltage loop
- PFC Partial feedforward** cancels the input voltage disturbances to input current caused by smaller boost inductor in FCML
- Buffer control** obtains phase and amplitude information from PFC

Experimental Verification

Total box-volume power density:	230 W/in ³
Peak efficiency:	98.9%
1.5 kW efficiency:	98.1%
THD:	< 5%
Power factor:	> 0.994



Experimental waveforms demonstrating power factor correction, multi-level switching, and SSB @ 1.5 kW, 240 Vac to 400 Vdc

References:

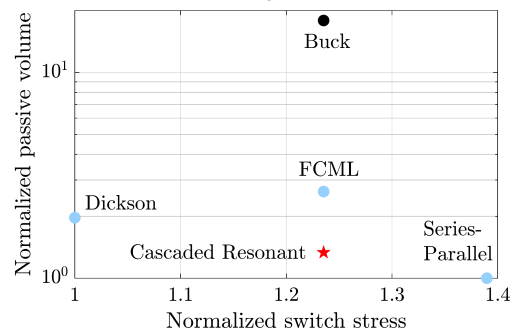
- Z. Liao, N. C. Brooks, and R. C. N. Pilawa-Podgurski, "A high power density power factor correction converter with a multilevel boost front-end and a series-stacked energy decoupling buffer," in 2018 IEEE Energy Conversion Congress and Exposition (ECCE), 2018
- Z. Liao, et al. "Multi-objective optimization of series-stacked energy decoupling buffers in single-phase converters," in 2018 IEEE19th Workshop on Control and Modeling for Power Electronics (COMPEL), July 2018, pp. 1-7.



High Efficiency High Power Density Hybrid/Resonant Switched-Capacitor Converter



Theoretical Analysis



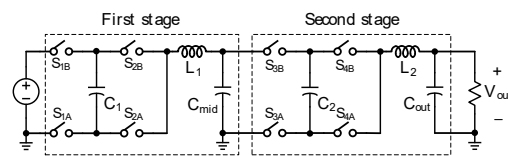
- Systematically analyze and calculate switch and passive utilization
- Compare and select the most suitable topology depending on application and power level
- Develop control technique to achieve soft-charging and soft-switching

Switch VA rating

$$\left(\sum_{switches} V_{ds} I_{ds} \right)$$

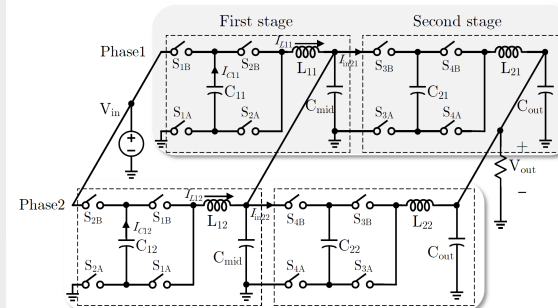
Total passives volume

$$\left(\frac{1}{2} \sum C V^2 + \frac{1}{2} \sum L I^2 \right)$$



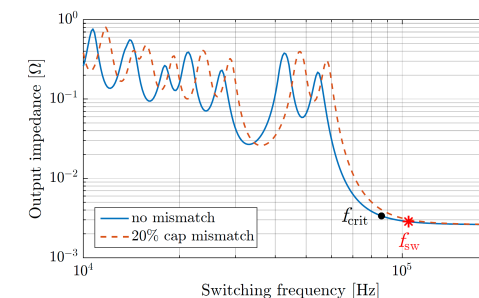
Cascaded Resonant Converter

Two-phase interleaved design



- Overcome the intermediate decoupling challenge of doubler topology

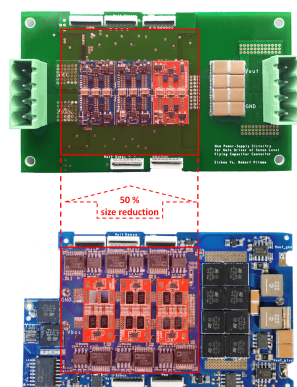
Zero voltage switching technique



- Operate the tank in the inductive region to achieve ZVS, while improving tolerance of component variations

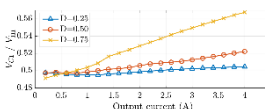
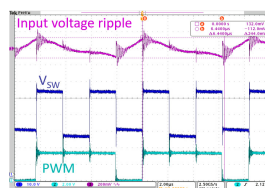
Practical Challenges and Solutions

Floating gate drive



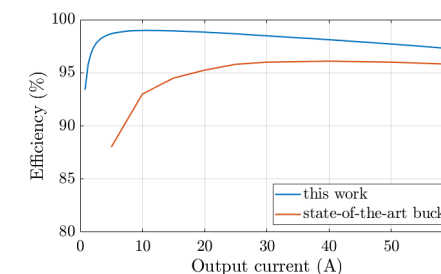
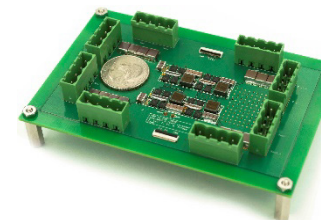
- Improved bootstrap and charge pump techniques to replace isolated dc/dc power supplies
- Achieving higher efficiency, lower cost and smaller footprint
- Working on system level circuit integration to further reduce size and cost

Capacitor voltage balancing

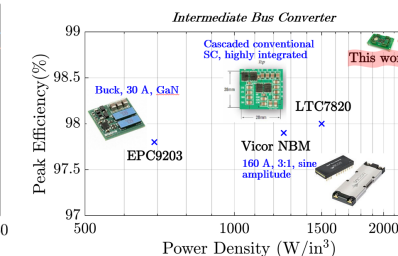


- Experimentally verified that source impedance and input capacitance can affect balancing drastically
- Even-level FCML converter has better natural balancing
- Gate drive voltage and signal mismatch can cause imbalance

Experimental Verification



Comparison with state-of-the-art



References:

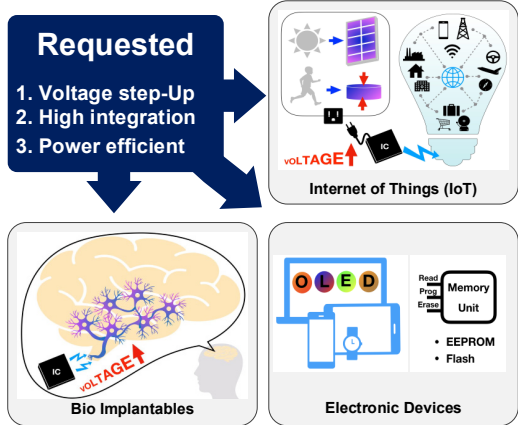
- [1] Z. Ye, Y. Lei, W. Liu, P. S. Shenoy and R. C. N. Pilawa-Podgurski, "Design and implementation of a low-cost and compact floating gate drive power circuit for GaN-based flying capacitor multi-level converters," *APEC 2017*
- [2] Z. Ye, Y. Lei, Z. Liao and R. C. N. Pilawa-Podgurski, "Investigation of capacitor voltage balancing in practical implementations of flying capacitor multilevel converters", *COMPEL 2017*
- [3] Z. Ye, Y. Lei and R. C. N. Pilawa-Podgurski, "A resonant switched capacitor based 4-to-1 bus converter achieving 2180 W/in³ power density and 98.9% peak efficiency," *APEC 2018*



An 83mA 96.8% Peak Efficiency On-Chip 3-Level Boost Converter with Full-Range Auto-Capacitor-Calibrating Pulse Frequency Modulation (ACC-PFM)



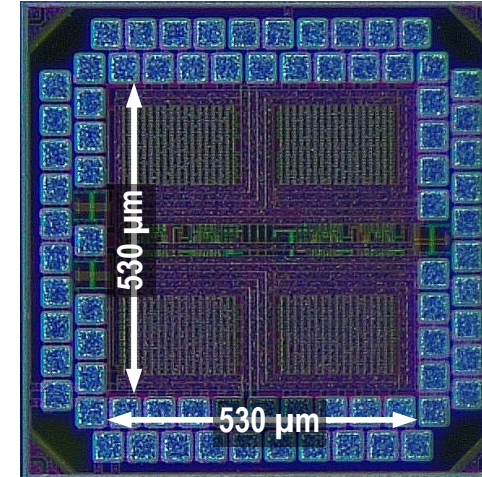
Motivation and Applications



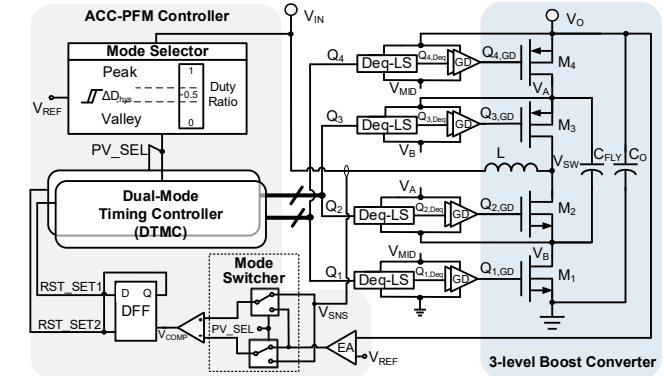
High voltages are demanded to

- Generate efficacious stimulations for bio-implantable devices
- Interface between low-voltage energy harvesters and batteries for wireless sensor network (WSN)
- Program memories for high operational speeds
- Drive LED strings efficiently

Chip Implementation

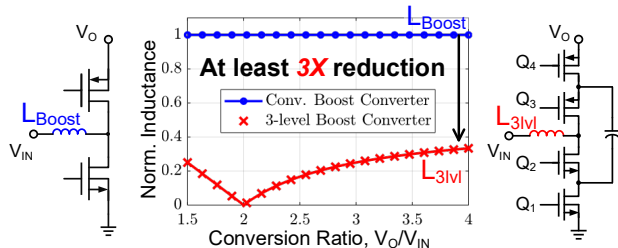


- TSMC 65nm CMOS process
- 2.5V devices for 5.0V operation



Challenges and Solutions

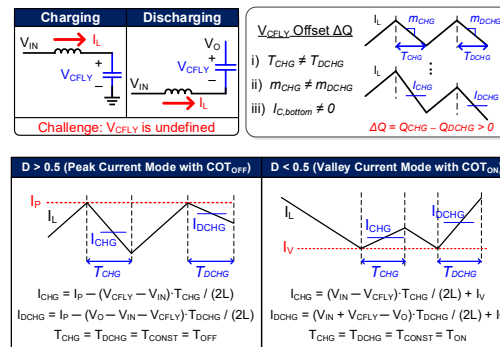
Topology: 3-level Boost Converter



Hybrid SC converters merge the advantages of the conventional switched capacitor (SC) and switched inductor converters (e.g. Boost converter)

- Achieve high power density
- Mitigate charge sharing loss in SC converter
- Retain the ability to employ low voltage

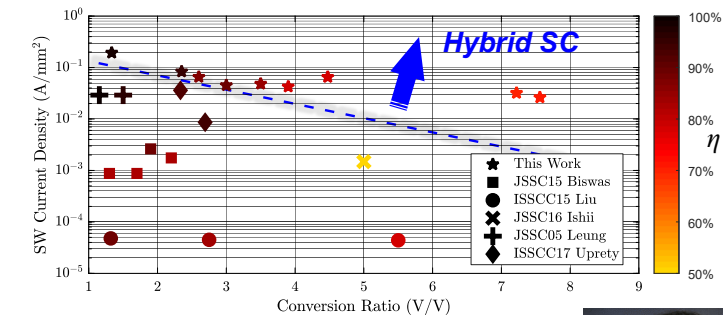
Control: ACC-PFM



- ACC-PFM is an integrated controller solution for both V_{OUT} regulation and capacitor balancing

Measurement Results

Peak Efficiency	96.8%
Input Voltage	0.3 – 3V
Output Voltage	2.4 – 5V
Peak Output Current	83 mA
Peak Switch Current Density	300 mA/mm ²
Switching Freq.	0.5M – 45MHz

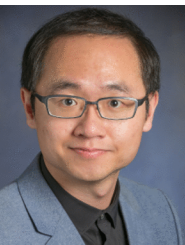


Excellent performance for wide-range voltage and load variation required in step-up applications, compared to prior arts.

References:

Wen-Chuen Liu, Pei Han Ng, Robert C.N. Pilawa-Podgurski, "An 83mA 96.8% Peak Efficiency 3-Level Boost Converter with Full-Range Auto-Capacitor-Calibrating Pulse Frequency Modulation", *IEEE Custom Integrated Circuits Conf. (CICC)*, 2019.

Student: Wen-Chuen Liu Email: joseph.wliu@berkeley.edu



A 94.2%-peak-efficiency 1.53A direct-battery-hook-up hybrid Dickson switched-capacitor DC-DC converter with wide continuous conversion ratio in 65nm CMOS



Berkeley Power and Energy Center

Motivation and Application

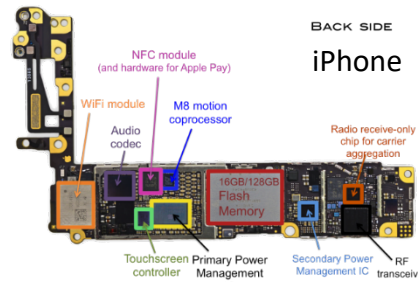
Increased power density of advanced CMOS nodes in embedded applications requires the power converters to have:

- Higher efficiency to extend the battery life
- Low loss to ease the thermal management
- Higher power density to match the technology
- Maintain performance at large conversion ratios

Typical Battery voltage 3.2 V to 4.2 V

Typical Load voltage 300m V to 1 V

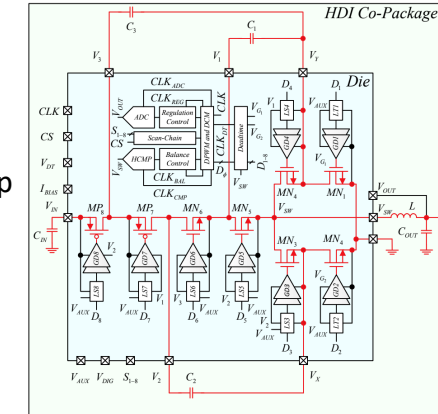
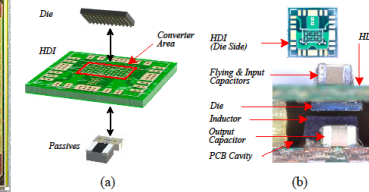
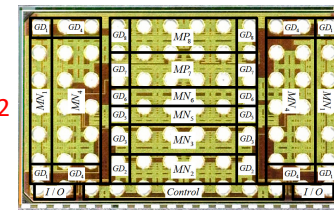
Typical Load current several mA to several A



Hardware

- Implemented in CMOS 65nm bulk process
- Flip-Chip packaging for low parasitic
- Voltage borrowing gate drive to eliminate bootstrap capacitors and increase power density
- Active capacitor balancing and output regulation
- External flying capacitors and inductor
- High density interposer for uModule assembly

Die 4 mm²



System Architecture

uModule Assembly

Challenges and Solutions

Utilized hybrid switched-capacitor (SC) converters.

Switched-Capacitor stage:

- Higher efficiency at large conversion ratios
- Lower rated devices for advance CMOS integration
- Poor regulation

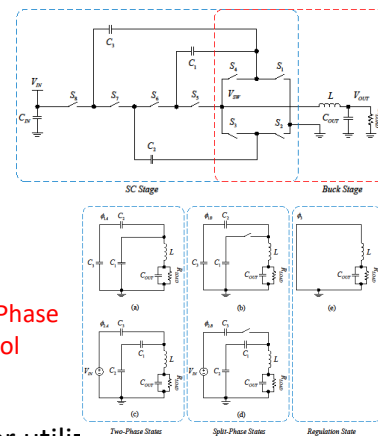
Magnetic Buck stage:

- Achieve tighter regulation
- Lower voltage swing for smaller magnetics

Need higher utilization of passive and active devices:

- Dickson SC has good switch utilization and poor capacitor utilization
- Soft-charging through split-phase control increases capacitor utilization, enhances efficiency and lower switching frequency
- Smaller passives for faster transient response and tighter control

4:1 Hybrid Dickson

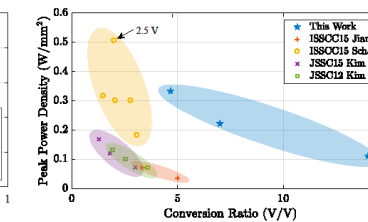
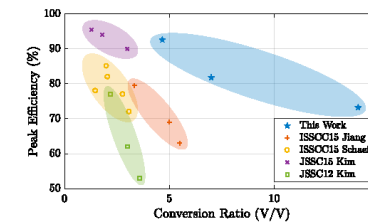
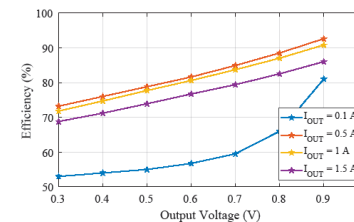


Split-Phase Control

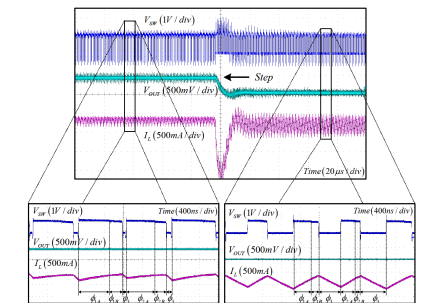
Experimental Verification

Maintained efficiency and power density:

- Across large conversion ratios
- Across large load current range

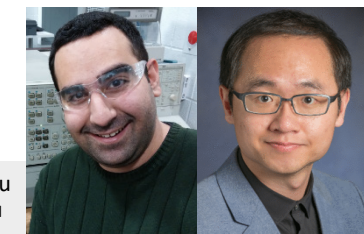


Output regulation and flying capacitor active balancing



Reference: W. Liu, P. Assem, Y. Lei, P. K. Hanumolu and R. Pilawa-Podgurski, "10.3 A 94.2%-peak-efficiency 1.53A direct-battery-hook-up hybrid Dickson switched-capacitor DC-DC converter with wide continuous conversion ratio in 65nm CMOS," *ISSCC 2017*.

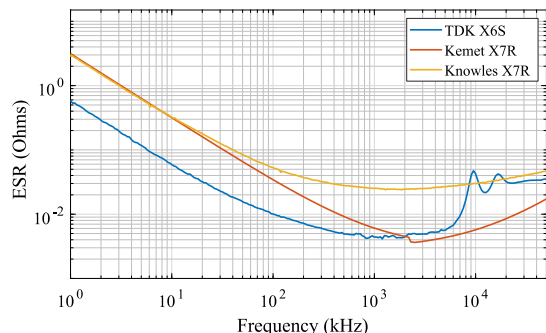
Pourya Assem: pourya_assem@Berkeley.edu
Wen-Chuen Liu: joseph.wliu@Berkeley.edu



Characterization of Multi-layer Ceramic Capacitors under More Realistic Operating Conditions



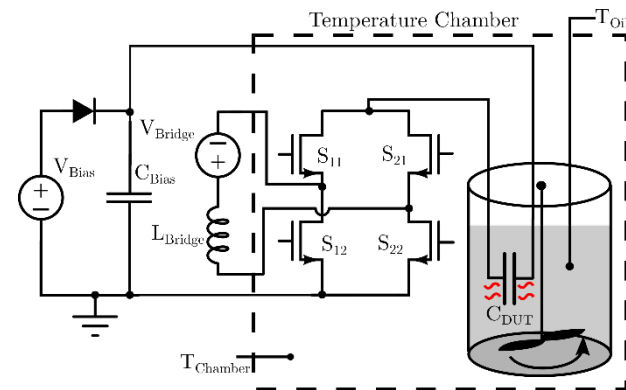
Motivation and Applications



- Multi-layer ceramic capacitors (MLCCs) are a key enabling technology for high density power converters.
- Real losses in MLCCs can be reduced to equivalent series resistance (ESR)
- Data sheets do not provide loss information for realistic operating conditions.

Hardware Implementation

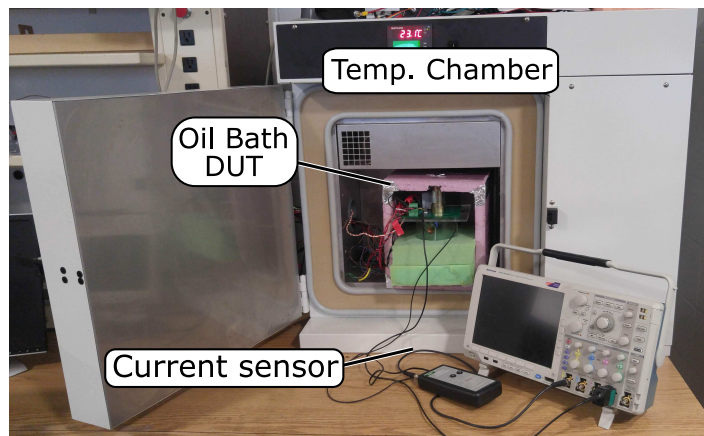
- ESR is dependent on frequency, DC bias, AC amplitude, temperature and harmonic content.
- A circuit was designed to be able to adjust frequency, current amplitude and DC bias of a high harmonic content waveform in order to test the effect on ESR.



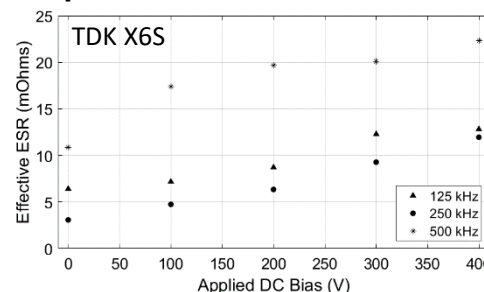
Challenges and Solutions

$$P_{diss} = \frac{1}{T_{final}} \left(k_{oil} \Delta temp + \int_0^{T_{final}} \frac{temp_{oil} - temp_{amb}}{R} dt \right) [1]$$

- Measuring loss with electrical characterization is inaccurate under desired operating conditions.
- A calorimetric method was implemented in order to accurately observe change in ESR.



Experimental Results



Capacitor Manufacturer	Capacitor Derating (at 400 V)	ESR increase (at 400 V, 125 kHz)
TDK	80%	200%
Knowles	82%	243%
Kemet	72%	142%

- With increased DC bias, the ESR linearly increases, this has been shown with several dielectric types as well as manufacturers.

References:

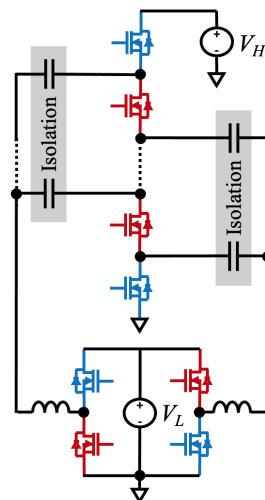
[1] G. S. Dimitrakakis, E. C. Tatakis, and A. C. Nanakos, "A simple calorimetric setup for the accurate measurement of losses in power electronic converters," *EPE 2011*.
 [2] S. Coday, C. B. Barth and R. C. N. Pilawa-Podgurski, "Characterization and Modeling of Ceramic Capacitor Losses under Large Signal Operating Conditions," *COMPEL 2018*.

Student: Samantha Coday
 Email: scoday@berkeley.edu



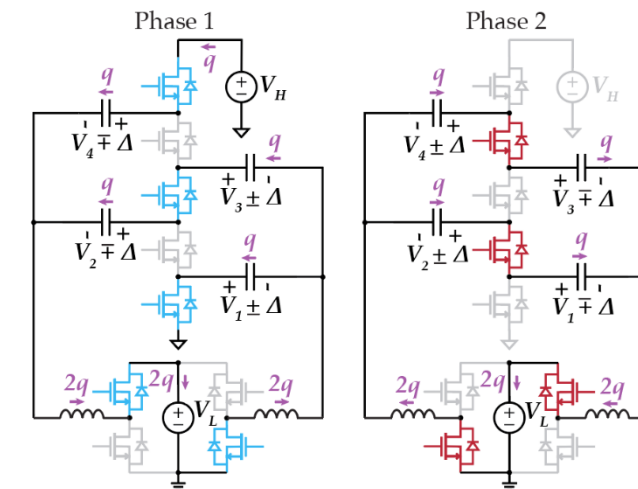
Motivation and Applications

- Hybrid switched-capacitor converters offer high power density but have been restricted to non-isolated applications
- Traditional isolation methods require bulky and heavy transformers
- Capacitive isolation presents a power-dense alternative to magnetic isolation
- Flying capacitors with high voltage rating act as isolation capacitors



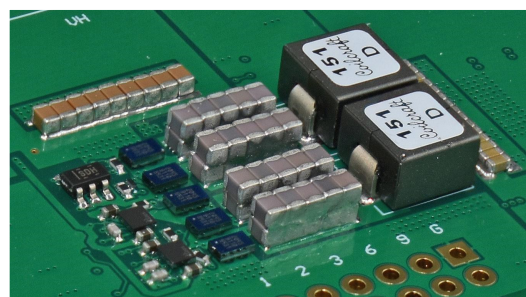
Theory of Operation

- Capacitively isolated hybrid switched-capacitor converter based on [1], [2]
- Complete soft-charging of capacitors eliminates loss from transient inrush currents
- 50% duty cycle and two-phase operation
- Switch voltage stress independent of load



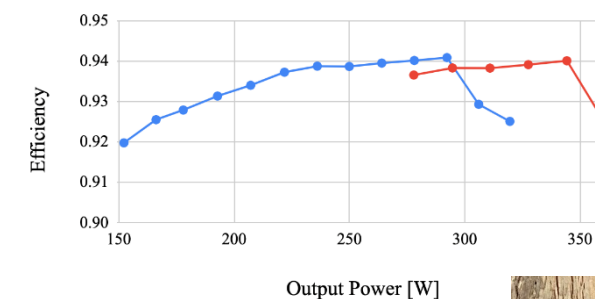
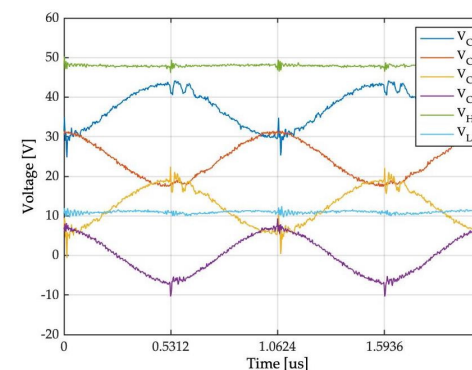
Challenges and Solutions

- ZVS theoretically possible, but not successful at higher input voltages
 - Ongoing issue; we'll spend more time investigating timing
- Light-load oscillations that damage converter at higher voltages
 - Current solution: avoid light load



Experimental Results

- 94.1% peak efficiency, 2,010 W/in³ power density



[1] Y. Li, L. Gu, A. Hariya, Y. Ishizuka, J. Rivas-Davila, and S. Sanders, "A wide input range isolated stacked resonant switched-capacitor dc-dc converter for high conversion ratios," in *2018 IEEE 19th Workshop on Control and Modeling for Power Electronics (COMPEL)*, 2018, pp. 1–7.

[2] N. M. Ellis and R. Amiratharajah, "A resonant dual extended lc-tank dickson converter with 502021 *IEEE Applied Power Electronics Conference and Exposition (APEC)*, 2021, pp. 1282–1287.

Core Size Scaling Law of Two-Phase Coupled Inductors – Demonstration in a 48-to-1.8 V MLB (Multi-Level-Binary)-PoL Converter

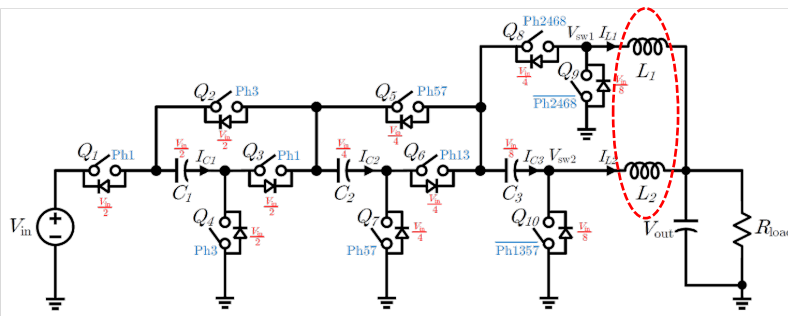


Berkeley Power and Energy Center

Motivation and Applications

Multi-Level Binary (MLB) hybrid switched-capacitor converter for 48 V to PoL conversion

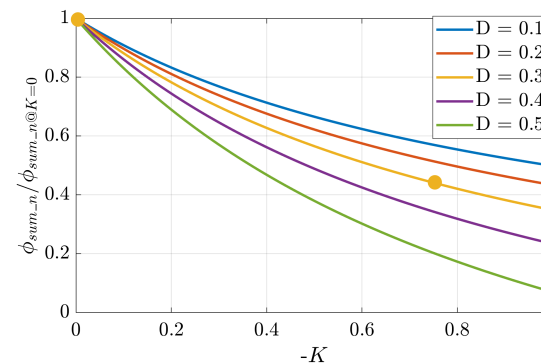
- In Point-of-Load (PoL) applications, inductors usually occupy >50% total volume
- A general core-size model** is desired to evaluate the duty-ratio advantage of hybrid converters and guide magnetic design



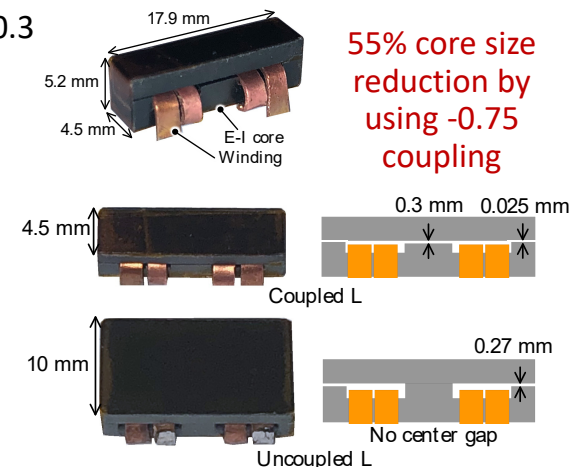
Zichao Ye, 2020 COMPEL

Hardware Implementation

Modeled $\Phi_{sum_n} / \Phi_{sum_n@K=0}$ versus $-K$ at $\alpha = 0.3$



K: coupling coefficient



55% core size reduction by using -0.75 coupling

Proposed Method and Result

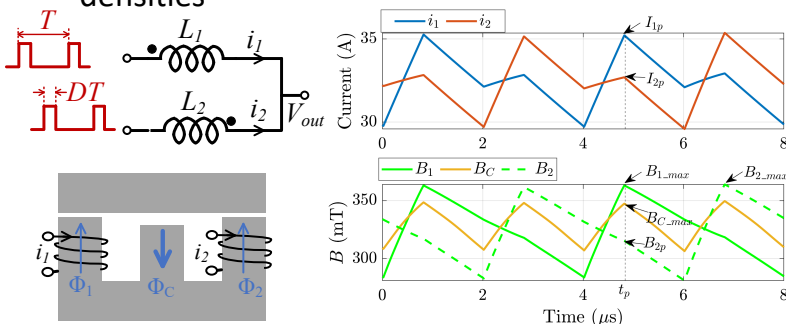
- 2-phase coupled inductors: schematic, core structure, current waveforms, and flux densities

- Total flux is proportional to core size and calculated by:

$$\begin{bmatrix} \Phi_{1_max} \\ \Phi_{2p} \end{bmatrix} = \begin{bmatrix} L_s & KL_s \\ KL_s & L_s \end{bmatrix} \begin{bmatrix} I_{1p} \\ I_{2p} \end{bmatrix} / N$$

$$\Phi_{sum_N} = \frac{\Phi_{sum} f_{sw} N}{V_{out}}$$

$$= \frac{4}{\alpha(1-K)} - \left(\frac{4}{\alpha} + 2 \right) D + \frac{3}{2}$$



α : ripple factor, defined by the peak-to-peak inductor current over the maximum dc current

Reference: T. Ge, R. Abramson, Z. Ye, and R. C. N. Pilawa-Podgurski, "Core Size Scaling Law of Two-Phase Coupled Inductors – Demonstration in a 48-to-1.8 V Hybrid Switched-Capacitor MLB-PoL Converter," 2022 APEC.

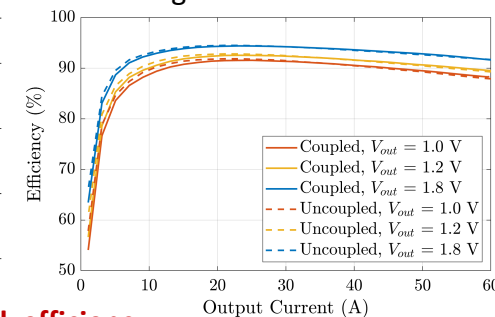
Experimental Results

Converter specifications	
V_{in}	48 V
Max. V_{out}	1.8 V
Max. D	0.3
Max. I_{out}	65 A
f_{sw}	250 kHz
α	0.3
Design 1: coupled inductors	
K	-0.75
L_s	800 nH
Design 2: uncoupled inductors	
L	517 nH

Converter performance summary

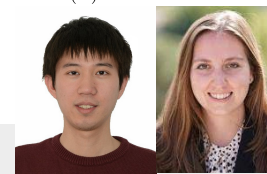
	Efficiency at 48 V input and 1.8 V output	Power density & Dimensions
Coupled L (This work)	Peak: 94.4% Full load: 91.5%	474 W/in ³ 26 × 18.4 × 7.8 mm
Uncoupled L (This work)	Peak: 94.5% Full load: 91.6%	391 W/in ³ 31.5 × 18.4 × 7.8 mm
[1] using commercial discrete L	Peak: 94.0% Full load: 91.3%	329 W/in ³ 29 × 18.4 × 10.1 mm

Measured efficiency including gate drive loss

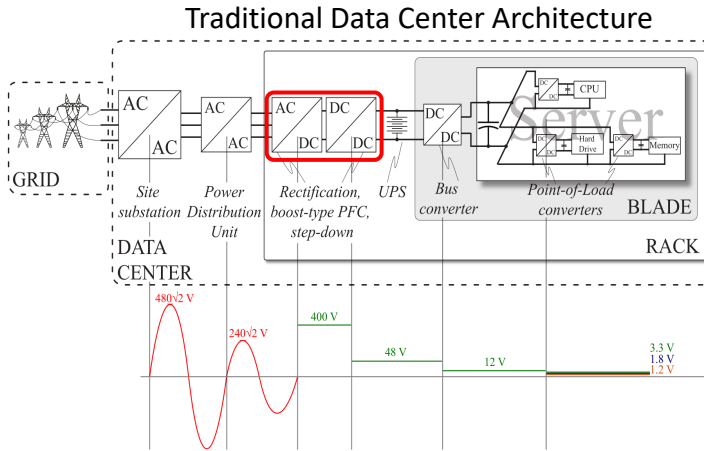


The converter with coupled L achieves **0.4% higher peak efficiency** and **44% higher power density** compared to the discrete counterpart.

Ting Ge, Rose Abramson Email: {tging, rose_abramson}@berkeley.edu



Motivation and Application

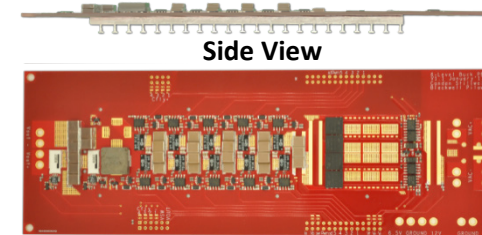


Traditional data center power factor correction (PFC) units boost voltage before rectification and step-down

Proposed: A one-stage single-phase ac-dc converter (240 Vac to 48 Vdc) with PFC

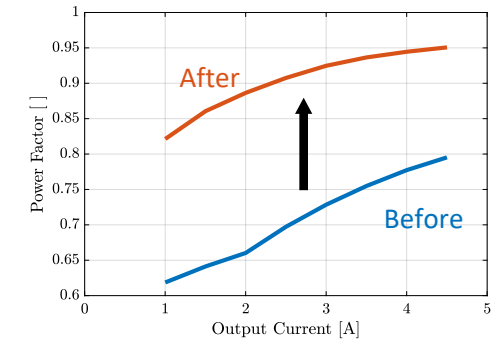
Metrics	Existing	Proposed
Peak Efficiency	94 %	97.8 %
Power Density	0.33 kW/L	7.5 kW/L

Hardware Prototype



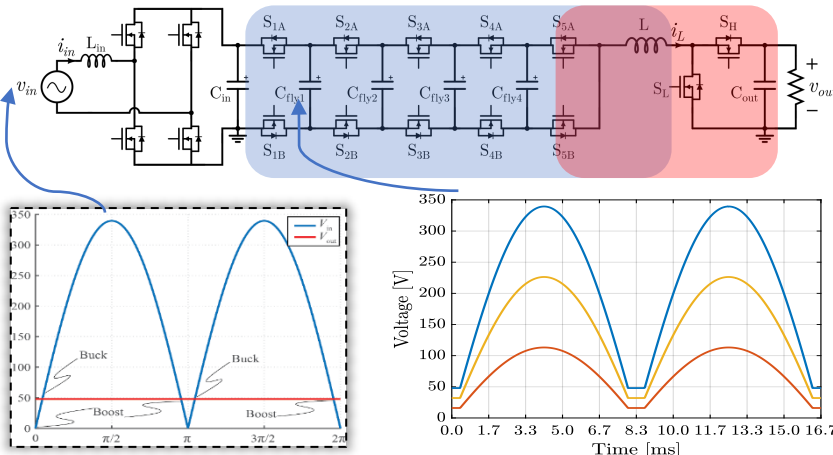
Operating Parameters	
Number of Levels	6
Switching Frequency	40 kHz
Output Current	4.5 A

Current Compensation to Improve Power Factor



Displacement current from C_{in} and C_{fly} leads to a phase shift in the input current, degrading the power factor. Our improved control algorithm compensates for this current to improve power factor [1].

Challenges and Solutions



Converter will buck or boost depending on point in AC input line cycle

Flying capacitor voltages vary with ac line cycle → unique challenges with capacitor balancing

Buck: S_H ON, S_L OFF; $S_{\{1,2,3,4,5\}A}$ and $S_{\{1,2,3,4,5\}B}$ modulate

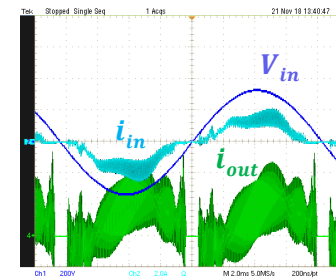
Boost: $S_{\{1,2,3,4,5\}A}$ ON, $S_{\{1,2,3,4,5\}B}$ OFF; S_L and S_H modulate

Preliminary prototype tests buck functionality, so that the converter is off when $|V_{in}| < V_{out}$.

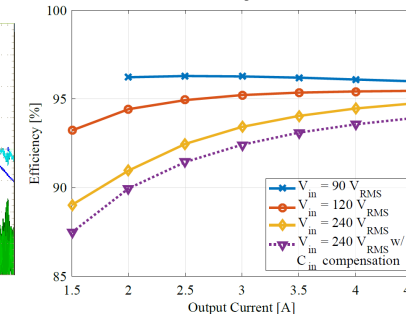
The converter relies on a stiff 48 V at the output (i.e. the UPS)

Experimental Verification

Operating Waveforms



Efficiency Curves



Performance Specifications

Efficiency	94.8% at 240 Vac, 250 W
Volume (Box)	2.45 in ³
Power Density	163 W/in ³ (w/o heatsink) 79 W/in ³ (w/ heatsink)

References:

[1] E. Candan, A. Stillwell, N. Brooks, R. Abramson, J. Strydom, R. C. N. Pilawa-Podgurski, "A 6-level Flying Capacitor Multi-level Converter for Single Phase Buck-type Power Factor Correction," in *Proceedings of 2019 IEEE Applied Power Electronics Conference and Exposition (APEC)*, March 2019.

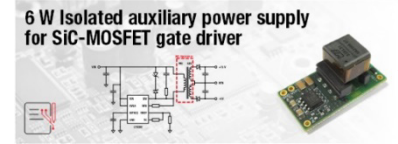


Advanced Techniques for Driving Floating Switches in the Flying Capacitor Multi-level converter

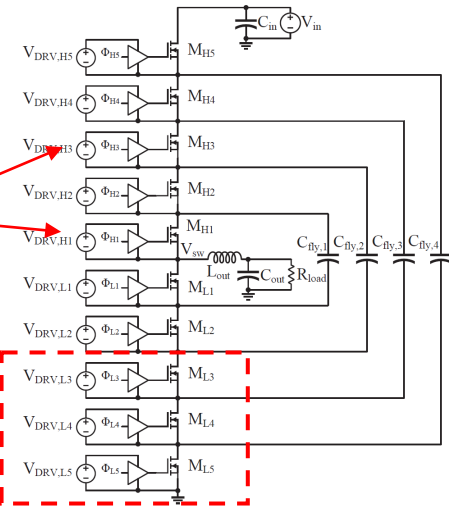
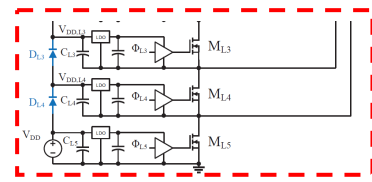
Motivation and Application

Floating switches need floating power supplies

- Typically use isolated power supply for each switch
- Large volume (due to isolation transformer) and high cost



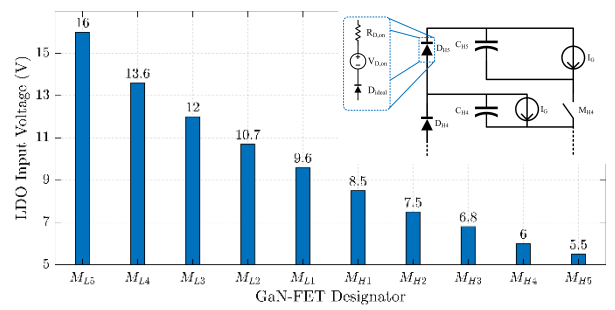
“Cascaded bootstrap” proposed for reduced volume and cost



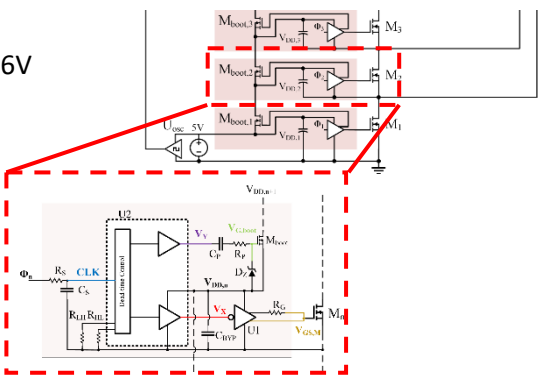
Challenges with Bootstrap Solution and Innovations

Voltage drops in bootstrap diodes require supply significantly higher than gate-drive voltage

- Local regulation necessary for driving GaN-FETs at 5-6V

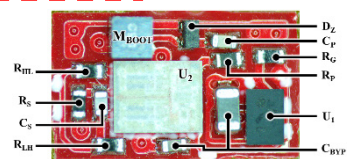


Synchronous Bootstrapping



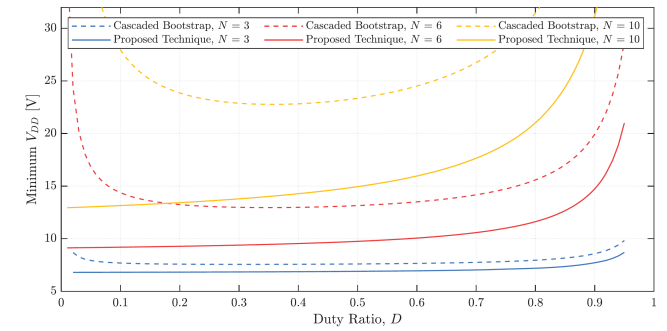
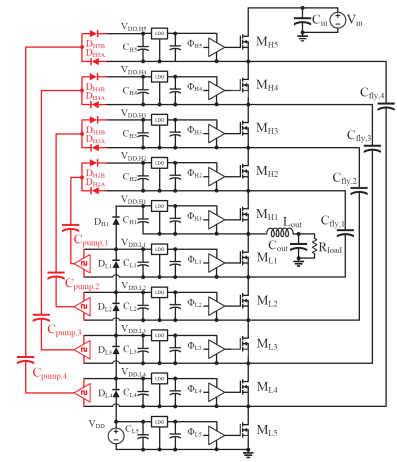
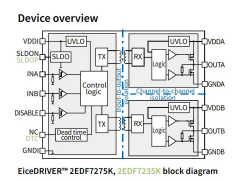
Replace bootstrap diodes with FETs

- Reduced voltage drop, bidirectional power delivery



Charge-Pump Technique

Oscillator driven charge pump: can be easily integrated with existing isolated drivers

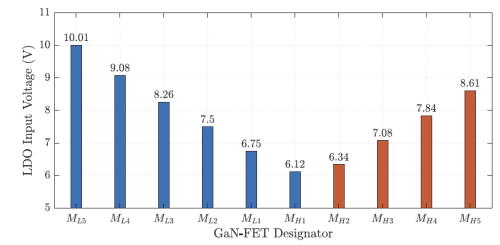


Can operate at low duty ratios with reduced gate-drive supply

- Higher gate drive efficiency

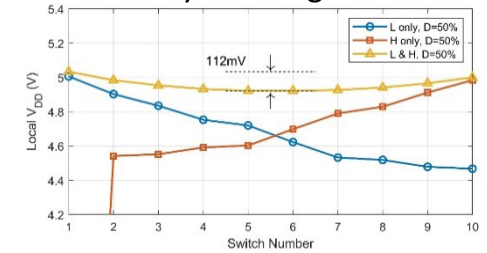
Experimental Verification

Reduced gate-drive supply with high-side switches fed by charge-pump



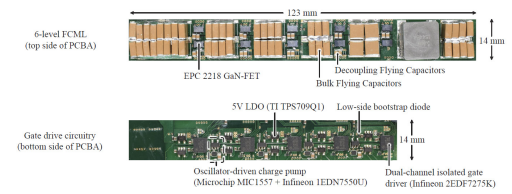
Synchronous bootstrapping:

- power delivery from high and low-sides

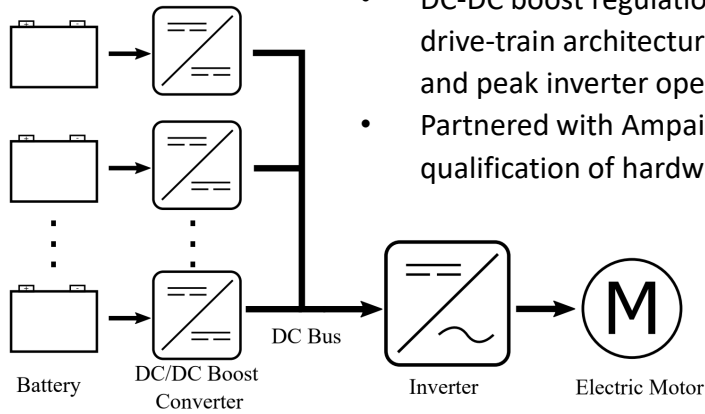


References:

- [1] Z. Ye, et al., "Improved Bootstrap Methods for Powering Floating Gate Drivers of Flying Capacitor Multilevel Converters and Hybrid Switched-Capacitor Converters," in IEEE Transactions on Power Electronics.
- [2] R. K. Iyer, N. M. Ellis, Z. Ye and R. C. N. Pilawa-Podgurski, "A High-Efficiency Charge-Pump Gate Drive Power Delivery Technique for Flying Capacitor Multi-Level Converters with Wide Operating Range," 2021 IEEE Energy Conversion Congress and Exposition (ECCE).
- [3] N. M. Ellis, R. Iyer and R. C. N. Pilawa-Podgurski, "A Synchronous Boot-strapping Technique with Increased On-time and Improved Efficiency for High-side Gate-drive Power Delivery," 2021 IEEE Workshop on Wide Bandgap Power Devices and Applications in Asia (WIPDA Asia)



Motivation and Application



Proposed drivetrain architecture.

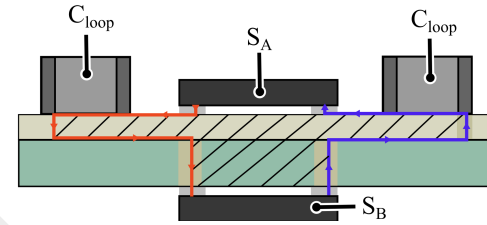
- DC-DC boost regulation stage added to hybrid electric drive-train architecture to allow variable battery voltage and peak inverter operation.
- Partnered with Ampaire and ARPA-E for flight qualification of hardware.



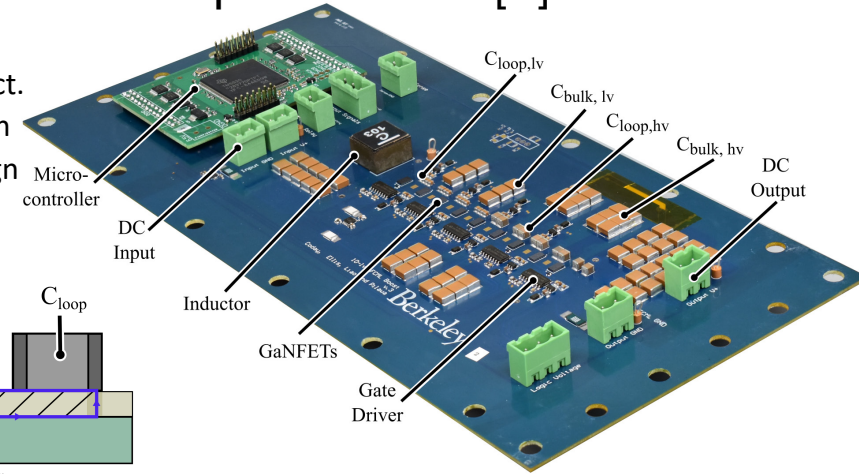
Ampaire EEL flight.

Hardware Implementation [1]

- 10-level FCML design is light-weight and compact.
- Modified electrically thin commutation loop design decreases parasitic inductance.

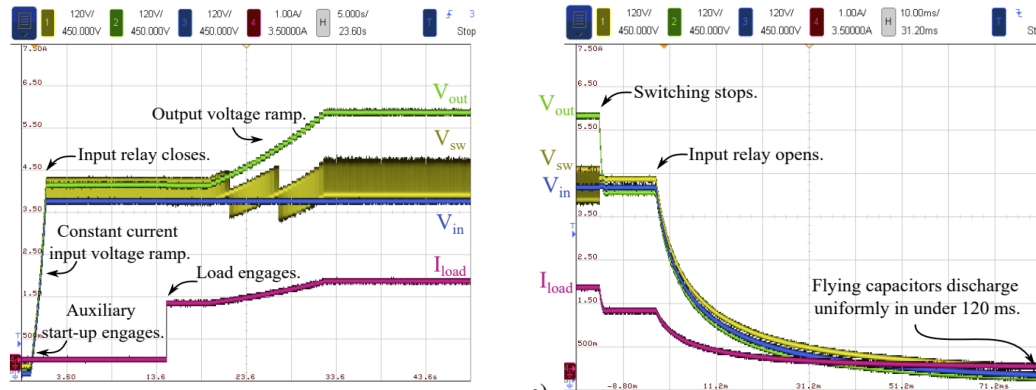


Commutation loop rendering.



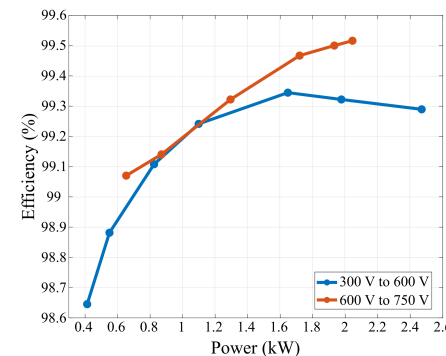
10-level FCML labelled hardware prototype.

Challenges and Solutions [2]

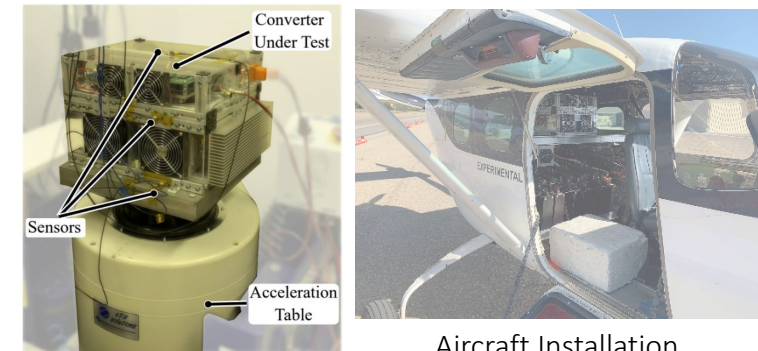


- Start-up auxiliary circuit and control allows for safe start-up at high voltages.
- Careful shutdown control of FCML is demonstrated as to not over stress switches.

Experimental Results [3]

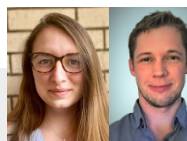


Measured efficiency (including gate drive losses).



Vibration test set-up.

Aircraft Installation



[1] S. Coday, N. Ellis, Z. Liao, and R. C. N. Pilawa-Podgurski, "A Lightweight Multilevel Power Converter for Electric Aircraft Drivetrain," in 2021 IEEE Energy Conversion Congress and Exposition (ECCE), 2021.

[2] S. Coday, N. Ellis, Z. Liao, and R. C. N. Pilawa-Podgurski, "Modeling and Analysis of Shutdown Dynamics in Flying Capacitor Multilevel Converters.," 2021 IEEE Workshop on Control and Modeling for Power Electronics (COMPEL), 2021.

[3] S. Coday, N. Ellis, N. Stokowski, and R. C. N. Pilawa-Podgurski, "Design and Implementation of a (Flying) Flying Capacitor Multilevel Converter," in 2022 IEEE Applied Power Electronics Conference and Exposition (APEC), 2022.